ADVANCED PHYSICS LABORATORY

XRF

X-Ray Fluorescence: Energy-Dispersive Technique (EDXRF)

PART II

Optional Experiments

Author: Natalia Krasnopolskaia
Last updated: N. Krasnopolskaia, January 2017

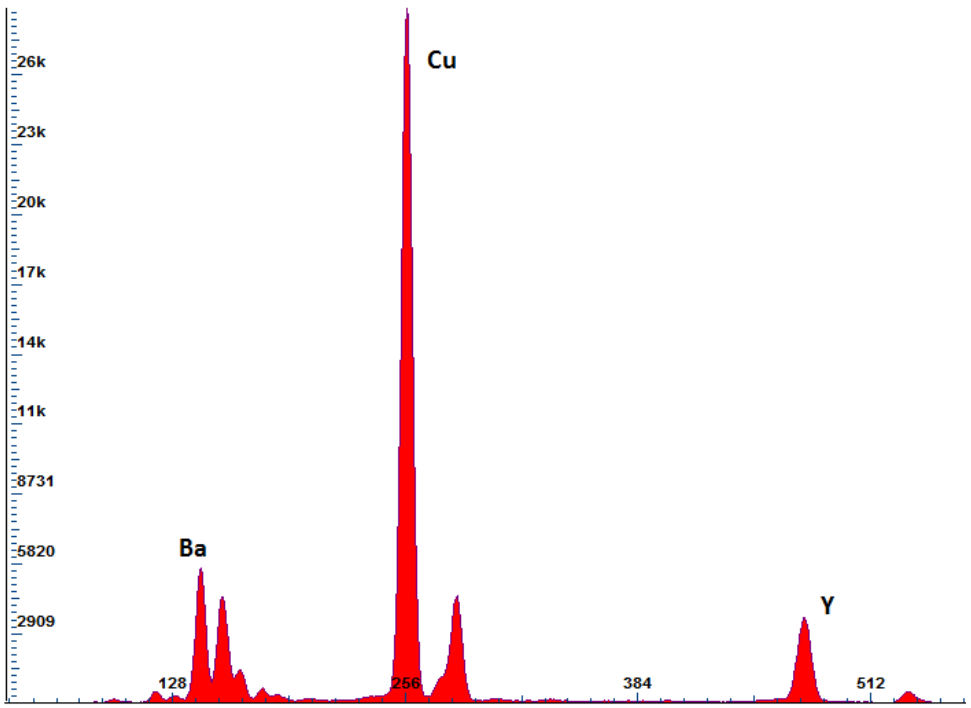

Spectrum of YBCO superconductor obtained by Oguzhan Can.
SURF 2013

Contents

INTRODUCTION

In Part I of the experiment you got familiar with fundamental ideas about the origin of x-ray photons as a result of decelerating of electrons in an x-ray tube and photoelectric effect in atoms of the x-ray tube and a target. For practical purposes, the processes in the x-ray tube and in the sample of interest must be explained in detail.

An X-ray photon from the x-ray tube incident on a target/sample can be either absorbed by the atoms of the target or scattered. The corresponding processes are:

(a) photoelectric effect (absorption) that gives rise to characteristic spectrum emitted isotropically;
(b) Compton effect (inelastic scattering; energy shifts toward the lower value); and
(c) Rayleigh scattering (elastic scattering; energy of the photon stays unchanged).

Each event of interaction between the incident particle and an atom or the other particle is characterized by its probability, which in spectroscopy is expressed through the cross section σ of the process. Actually, σ has a dimension of $[L^2]$ and in atomic and nuclear physics has a unit of *barn*: 1 barn = 10^{-24}cm^2. The dimensionless value of probability of a process is obtained by dividing σ by an effective cross section of a beam of radiation that generates the corresponding process.

I. X-Ray Fluorescence Due to Photoelectric Effect

The probability of photoelectric effect P_{pe} is equal to σ_{pe} / S_b , where σ_{pe} is the *photoelectric effect cross-section*, and S_b is the cross-sectional area of the beam of photons (from the x-ray tube in our experiment). The more useful definition of the cross section of photoelectric effect per one atom is the following:

$$\sigma_{pe} = \frac{\Delta N_{pi} / \Delta t}{\left(\frac{\Delta N_{ph}}{\Delta t}\right)\left(\frac{N_a}{S_b}\right)}, \qquad (1)$$

where $\Delta N_{pi} / \Delta t$ is the number of photoionizations per unit of time; $\Delta N_{ph} / \Delta t$ is the number of incident photons per unit time; and N_a is the number of atoms of the target per unit of the cross-sectional area of the beam S_b. Because $\Delta N_{pi} / \Delta t$ is energy dependable, Eq.1 gives the cross section of photoionization by photons of particular energy, i.e. the *monoenergetic* photons. It is a usual practice in x-ray spectrometry to derive analytical equations for x-ray excitation by monoenergetic radiation with further integration over the range of energies represented in the incident beam of particles (photons, protons, electrons, etc.). Note: the photoelectric effect can take place only if the energy of the incident photon exceeds the binding energy of the electron. The minimum energy of the incident photon to create a vacancy in an electron shell is called the *absorption edge of the shell.*

In on average 10^{-8} s, the photoionization is followed by transition of the outer shell electron to the vacancy in the inner shell accompanied by one of two competing processes: 1) the emission of characteristic X-rays with probability p_r ; or 2) emission of the other electron from an outer shell (this phenomenon is called Auger effect) with probability p_A. Thus the probability of fluorescence is given by *fluorescence yield* ω

$$\omega = \frac{p_r}{p_r + p_A} \quad ,$$

which may be calculated with a number of proposed functions of approximation or obtained experimentally [1] (see APPENDIX D for fluorescence yields of chemical elements).

The transitions leading to X-ray fluorescence emission are governed by selection rules ($\Delta\ell = \pm 1$ and $\Delta j = \pm 1, 0$) between various electronic states of an atom. Every transition occurs with a definite *transition probability* p_{tr}. The value for p_{tr} in a particular atom is calculated theoretically and verified in experiment [2] (also see [3] and APPENDIX D for transition probabilities).

Fluorescence radiation, induced in the target by primary radiation of x-ray tube, can in turn be absorbed or scattered inside the target/sample. The processes that decrease the number of emitted photons are numerically characterized with attenuation coefficient for the emitted energy in a particular substance. Attenuation coefficient depends upon the energy of photons and absorption properties of atoms. A linear attenuation coefficient μ_l is defined as the relative loss of the number of photons on a unit of depth of the sample penetrated by the beam of photons:

$$\mu_l = \frac{-dN_x}{N_x \cdot dx}, \qquad (2)$$

where N_x is the initial number of photons incident on the differential layer of a target at a depth x; and dN_x is the number of lost photons of the beam after traveling through the layer of thickness dx. The unit of μ_l is cm^{-1}. Figure 1 depicts attenuation of incident radiation by a differential layer of a substance.

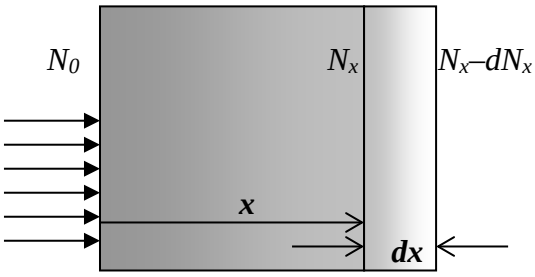

FIG.1: Attenuation of the incident beam of N_0 photons in a sample.

It appears more convenient to calculate attenuation with the mass attenuation coefficient, μ, given by $\mu = \frac{\mu_l}{\rho}$, where ρ is the density of the sample in g/cm^3. Eq.2 can be rewritten for the number of the lost photons in the layer dx using the mass attenuation coefficient as

$$-dN_x = N_x \mu \rho \, dx \qquad (3)$$

Solution of this equation for the number of photons that passed through the layer of thickness d, gives

$$N = N_0 e^{-\mu\rho d}$$

In your experiment, the primary beam from the x-ray tube and the exit beam of photons from the target are incident at some angle to the surface of the target. To account for attenuation with this geometry, one should know the incident and the exit angle, for example φ and ψ (Fig.2).

For monoenergetic photons, the number of primary beam photons that reach an element of the target at the depth d is

$$N_{1d} = N_{10} \exp(-\mu_{1t} \rho_t \, d / \cos\varphi), \qquad (4a)$$

and the number of characteristic photons of the element *i* that comes to the surface from the depth *d* is

$$N_{id} = N_{i0} \exp(-\mu_{it}\,\rho_t\, d / \cos\psi), \quad (4b)$$

where N_{10} is the number of primary photons incident on the surface of the target; μ_{1t} – the mass attenuation coefficient for the primary radiation in the target; ρ_t is the density of the material of the target; N_{i0} is the number of characteristic photons of the element *i* produced at the depth *d*; μ_{it} is the mass attenuation coefficient for the characteristic photons of the element *i* in the material of the target.

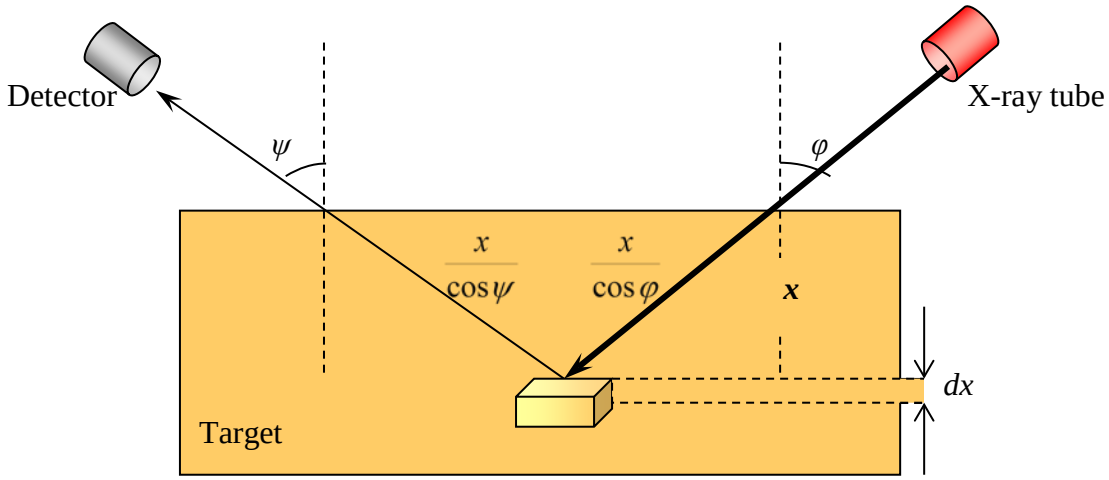

FIG.2: Arrangement of the x-ray tube, the sample (target) and the detector (all distances are not to scale).

For the multi-component target such as an alloy, the attenuation should be calculated as

$$\mu_{1t} = \sum_{j=1}^{n} \mu_{1j} C_j \quad \text{and} \quad \mu_{it} = \sum_{j=1}^{n} \mu_{ij} C_j \quad (5)$$

where C_j is the mass concentration of the element *j* in the target and *n* is the total number of chemical elements in the target.

Attenuation coefficient is responsible for all kinds of interactions between photons and atoms of the target and can be expressed in terms of cross sections of the processes as

$$\mu_{1i} = \left(\frac{\sigma_{pe} + \sigma_{Compton} + \sigma_R}{A} \right)_i N_A \quad (6)$$

where σ_{pe} is the photoelectric effect cross-section; $\sigma_{Compton}$ is the cross section for the Compton scattering; σ_R is the cross-section for coherent (Rayleigh) scattering; A_i is the atomic mass of the element *i* in g/mole; and N_A is Avogadro number. Other processes are not observed within the energy range of our experiment. Eq.6 contains the cross sections of interaction of monoenergetic photons of the primary beam with atoms of element *i* and can be obtained by combining Eqs.1 and 2 with definition of the mass attenuation coefficient. The attenuation coefficient can be easily measured experimentally; therefore, the probability and cross section of a particular process are usually substituted by attenuation coefficient or its fractions.

As the relationship among the photoelectric cross section, atomic number *Z* of an absorber and energy *E* of the photons is given by

$$\sigma_{pe} \propto \frac{Z^p}{E^q} \quad (7)$$

where $4 \le p \le 5$; and $q \approx 3$, it is clear that materials with greater Z are better absorbers (lead is the usual shielding material in laboratories with ionizing radiation); and the materials with small Z should be used when the minimum possible attenuation is required. The evacuated x-ray tube is separated from the environment by beryllium (Z = 4) window to reduce effect of attenuation. The cross section for a photoelectric absorption of a photon with energy E by the atom of element i can be replaced by the absorption coefficient $\tau_{1i}(E)$ as:

$$\sigma_{pei}(E) = \tau_{1i}(E)\frac{A_i}{N_A} \qquad (8)$$

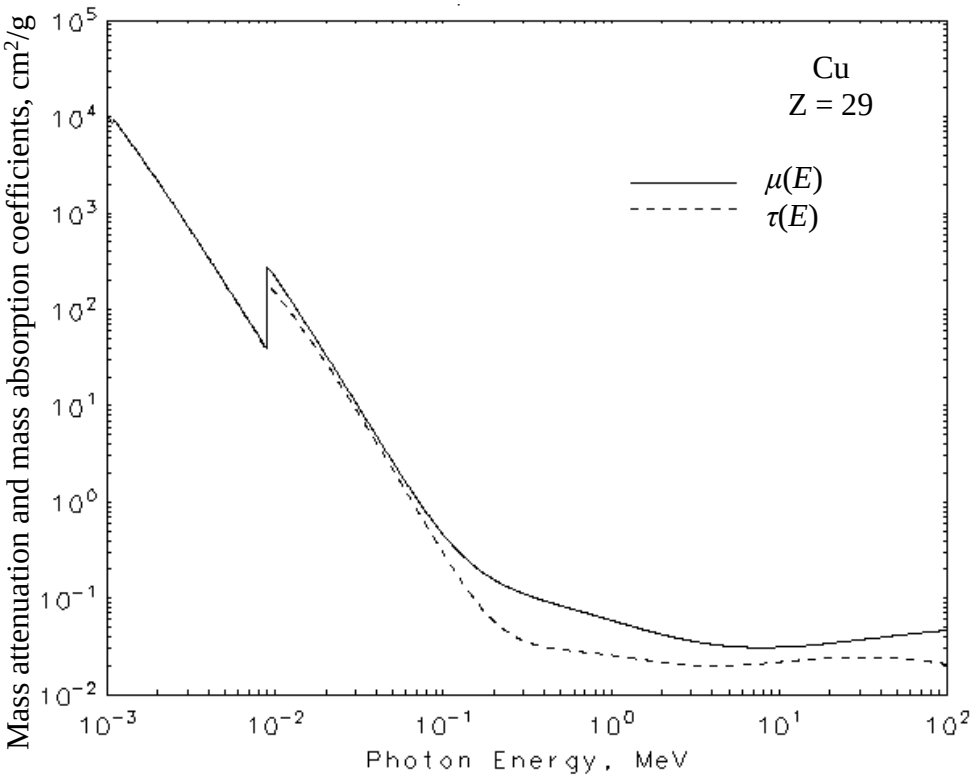

FIG. 3: Mass attenuation coefficient μ and mass absorption coefficient τ in copper (Cu).
[http://physics.nist.gov/PhysRefData/XrayMassCoef/ElemTab/z29.html]

Figure 3 shows that both coefficients experience "a jump" at the energy of absorption edge of the K-shell. The ratio of the absorption coefficients on the two sides of the absorption edge is called the *absorption edge jump ratio* and is designated as r_s for a specific subshell s (K, L_I, L_{II}, L_{III}, M_V, etc) [4]. It is related to absorption jump factor J_s as $J_s = 1 - \frac{1}{r_s}$ (9)

where J_s is a probability of photoionization of a specific subshell. Thus, the cross section $\sigma_{K\alpha i}(E)$ of emission of a $K_{\alpha 1}$ photon of element i is given by

$$\sigma_{K\alpha i}(E) = \sigma_{pei}(E)\, J_{Ki}\, \omega_{Ki}\, p_{L\text{-}K,i}\ , \qquad (10)$$

where $p_{L\text{-}K,i}$ is the probability of electron transition from L_{III}-subshell to K-shell of element i. The majority of handbooks provide information about the values of r_s and not for J_s.

The chain of events resulting in emission of characteristic x-rays by the atom of element i of the target may be represented by the following scheme:
1. In x-ray tube: thermionic emission from a cathode of x-ray tube → acceleration of electrons by voltage between the cathode and anode of the x-ray tube → deceleration of electrons in the anode with emission of continuous spectrum (*bremsstrahlung* radiation); and ionization of atoms

of the anode by direct impact with incident electrons with emission of characteristic spectrum of the atoms of the anode → emission of spectrum of the x-ray tube (see Fig.6 (b) of Part I) →
2. On the way from the tube to a target: propagating of photons of characteristic and continuous spectrum from the tube (a *primary beam* of radiation) through the air towards a target/sample accompanied by attenuation of the beam due to interaction with atoms of the air →
3. In the target: (a) attenuation of the primary x-ray beam in the target; (b) coherent and incoherent scattering of some part of the incident photons on the atoms of the target resulting in the spectrum *background*; (c) photoelectric excitation of atoms of the target by radiation with energy E exceeding the absorption edge of the corresponding atomic subshell with probability of $\sigma_i(E)\ J_s / S_b$ → emission of series of photons with probability of $\omega_i p_{tr\,i}$ → (d) emission of characteristic *secondary* radiation of atoms of the target generated by the characteristic radiation of other atoms of the target (matrix effects) → scattering and absorption of the secondary and *tertiary* radiation in the target which leads to attenuation of fluorescence and scattered radiation in the target →
4. On the way from the target to a detector: attenuation of the beam of radiation due to absorption in the air →
5. In the SiPIN diode: generation of pulses corresponding to the photons of different energy with amplitude proportional to the number of registered photons with specific energy →
6. In the Amptek XR100 spectrometer and PC: amplification and correction of a signal from the detector with converting it into the image on the PC monitor.

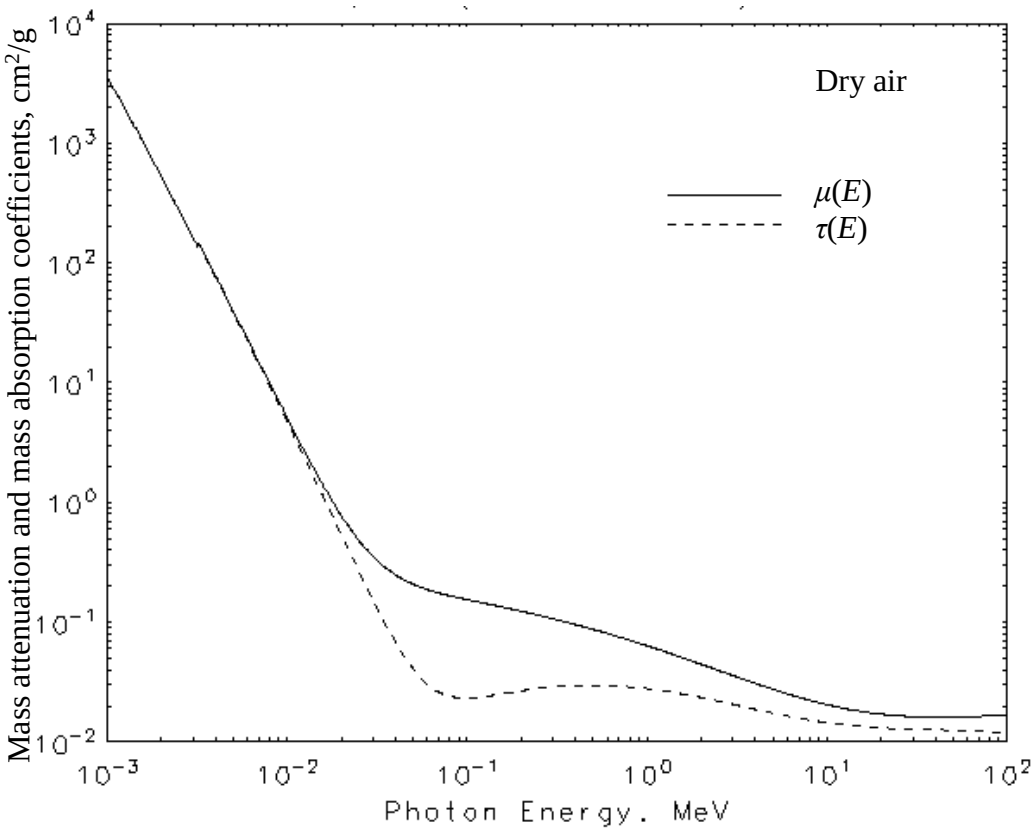

FIG.4: Mass attenuation coefficient μ and mass absorption coefficient τ in dry air.
[http://physics.nist.gov/PhysRefData/XrayMassCoef/ComTab/air.html]

Figure 4 gives an estimate for loss of primary and secondary radiation intensity due to the beam attenuation in the air. For precise experiments that demand determination of traces of elements, an x-ray tube together with a sample and detector should be placed into evacuated chamber.

Useful reminder:

1) ***Intensity of a beam of particles*** (photons, electrons, ions, etc) is the number of particles ΔN that penetrate the unit of a cross-sectional area A per unit of time, i.e. $\Delta N / (\Delta t\, A)$;
2) ***Intensity of radiation*** is energy that transferred through the unit of cross-sectional area per unit of time, i.e. $\Delta E / (\Delta t\, A)$;
3) ***Intensity of a peak*** in a spectrum is the area under the peak which is proportional to the total number of registered photons of the energy associated with the peak maximum.

As a first step, the number of registered photons will be derived under consideration that the primary beam consists of *monoenergetic* photons with energy from E to $E+ dE$. The number of monoenergetic photons of the primary radiation will be designated as $dN_1(E)$. Second simplification will be made with the primary and secondary beam geometry. Actually the beams cannot be treated as parallel rays but diverge in a solid angle. As the distance between the x-ray tube and the sample is much greater than the diameter of a spot on the target surface illuminated by the primary radiation, the angle of incidence φ can be considered constant. The distance between the target and the detector is smaller, but can also be considered much greater than the entry window of the detector. However, a geometric factor G identical for all chemical elements in the target should be included into an equation for spectrum intensity. For an element i the characteristic peak intensity dN_i is given by:

$$dN_i = G\varepsilon_i dN_1(E)\tau_{1i}(E)\rho C_i \omega_i p_{tri}\left(1-\frac{1}{r_i}\right)\int_0^d \exp\left[-\rho x\frac{\sum \mu_{1j}(E)C_j}{\cos\varphi}\right]\cdot\exp\left[-\rho x\frac{\sum \mu_{ij}C_j}{\cos\psi}\right]dx \quad (11)$$

where ε_i is the efficiency of the detector for energy of the characteristic peak; d is the thickness of the target, which is a smooth uniform tablet of average density ρ. Other quantities were described above.

In general, integration of Eq.11 over the thickness of the target results in

$$dN_i = G\varepsilon_i dN_1(E)\tau_{1i}(E)\rho C_i \omega_i p_{tri}\left(1-\frac{1}{r_i}\right)\frac{1-\exp\left[-\rho d\left(\frac{\sum \mu_{1j}(E)C_j}{\cos\varphi}+\frac{\sum \mu_{ij}C_j}{\cos\psi}\right)\right]}{\rho\left(\frac{\sum \mu_{1j}(E)C_j}{\cos\varphi}+\frac{\sum \mu_{ij}C_j}{\cos\psi}\right)} \quad (12)$$

For "thick" samples when $\exp\left[-\rho d\left(\frac{\sum \mu_{1j}(E)C_j}{\cos\varphi}+\frac{\sum \mu_{ij}C_j}{\cos\psi}\right)\right] << 1$, Eq.12 can be rewritten in a simpler way:

$$dN_i = G\varepsilon_i dN_1(E)\tau_{1i}(E)\rho C_i \omega_i p_{tri}\left(1-\frac{1}{r_i}\right)\frac{1}{\rho\left(\frac{\sum \mu_{1j}(E)C_j}{\cos\varphi}+\frac{\sum \mu_{ij}C_j}{\cos\psi}\right)} \quad (13)$$

Eq.13 is quite applicable for the experiments in the labs, because all samples meet the criterion of a "thick" sample. The further simplification of Eq.13 for the experiment in Advanced Physics Laboratory can be based on the equation $\varphi = \psi = 45^o$ which is recommended to diminish the scattering contribution into the spectrum intensity:

$$dN_i = \left(\frac{1}{\sqrt{2}}G\right)\cdot\left[\varepsilon_i \omega_i p_{tr,i}\left(1-\frac{1}{r_i}\right)\right]\frac{\tau_{1i}(E)C_i}{\sum \mu_{1j}(E)C_j + \sum \mu_{ij}C_j}\cdot\frac{dN_1(E)}{dE}dE \qquad (14)$$

where $\cos\varphi = \cos\psi = 1/\sqrt{2}$.
However, the formula for relationship between the analyte concentration C_i and the intensity of one of characteristic peaks of the element *i* is not yet derived, as the Eq.14 gives just a part of the peak intensity generated by monoenergetic primary photons with energy between *E* and *E* + *dE*. To obtain a useful formula, one should integrate Eq.14 over the range of energies of all primary photons incident on the target.

To integrate Eq.14, one must measure *G*, find $dN_1(E)/$d*E* as a function of primary beam energy for a specific x-ray source, and to find a good fit for the values of absorption $\tau_{1i}(E)$ and attenuation $\mu_{1j}(E)$ coefficients as functions of *E* (e.g. as in [5]). This method is not applicable to our experiment mainly because of unknown function $dN_1(E)/$d*E*, as the data of Fig. 6(b) of Part I are not tabulated.

To calculate characteristic peak intensity without integrating Eq.14, we will make reasonable approximations based on properties of specific samples and goals of analytical problem. Using a ratio of intensities of two different peaks will lower the uncertainty associated with measuring the geometry factor *G* and partly the uncertainty in $dN_1(E)/$d*E* function.

II. Compton Effect and Coherent Scattering

Intensities of incoherent (Compton) scattering component of a spectrum and coherent (Rayleigh) scattering component are proportional to cross sections of the processes. Eq.6 gives the total cross section σ_{tot} of interaction of the primary radiation with the atoms of the target as a sum of three cross sections: $\sigma_{tot} = \sigma_{pe} + \sigma_{Compton} + \sigma_R$. Coherent, or Rayleigh, scattering is sometimes called Thomson scattering. Figures 3 and 4 permit to conclude that for energies of the primary radiation below 100 keV, the absorption coefficient and the attenuation coefficient are almost equal and therefore, the contribution of scattering into the total attenuation is negligible. This is also observed with the spectra you obtained in the part I of the experiment. Spectra of different samples contained almost no background component and the characteristic peaks seemed to be symmetric and with no satellites. For a detailed theory of scattering on atomic electrons see [6].

Because of the dynamics of Compton scattering, incident X-rays below 50 keV in energy give rise to little or no K or L fluorescence from the middle-weight atoms. However, Compton scattering does produce a continuous background, especially at low *Z*, which cannot be observed with the spectrometer in our experiment.

The probability for a photon to scatter in a unit of a solid angle dΩ is called the differential probability and for two scattering processes the differential cross sections are given by [6]:

$$\frac{d\sigma_{Compton}}{d\Omega}(\theta,E) = \frac{r_e^2}{2}\left(\frac{k}{k_0}\right)^2\left(\frac{k}{k_0}+\frac{k_0}{k}-\sin^2\theta\right) \qquad (15)$$

$$\frac{d\sigma_R}{d\Omega}(\theta,E) = \frac{r_e^2}{2}\left(1+\cos^2\theta\right) \qquad (16)$$

where $\theta = \varphi + \psi$ is the scattering angle (see Fig. 2.); $r_e = \frac{e}{m_e c^2}$, which is the classical electron radius; *e* and m_e are the charge and the rest mass of the electron; and k_0 and *k* are the wave functions of the photon before and after the collision with an electron.

According to Eqs.15 and 16, the minimum value for differential cross sections is obtained for θ = 90°. That is why the mutual arrangement of the x-ray tube, the sample surface and the detector in your setup was designed with θ = 90°. Experimental results do not always confirm this conclusion and measurements of differential cross sections sometimes result in the minimum value at the angles 120° or 30° depending upon the energy of a photon scattered on an electron of a specific atom.
You can perform an optional set of experiments to study the structure of the x-ray spectrum and Compton Effect in the target in detail.

III. Difficulties in identification of characteristic peaks.

X-ray fluorescence spectrum in your experiment may be rather complicated, containing a number of overlapping peaks, superimposed on a background described by the unknown function. Each characteristic peak has a Gaussian shape, given by the function:

$$N(E) = N_0 \exp\left[-\frac{1}{2}\left(\frac{E-E_0}{\sigma}\right)^2\right] \qquad (15)$$

where E is energy associated with the channel of MCA, E_0 is the position of the maximum of the peak with the number of counts N_0, and σ is the standard deviation. This is a detector response function, which can be distorted under imperfect condition of the experiment or as a result of wrong settings. Sometimes, the Gaussian peak becomes skewed because of extremely high counting rate, or appearance of a Compton peak due to a specific sample orientation in the chamber.

Qualitative fluorescence analysis of a sample is pretty simple when characteristic peaks of different elements are well resolved which means that their maxima are at a distance exceeding the value of FWHM for this range of the spectrum. The quantitative analysis, however, can be perfectly run only when a maximum of the nearest characteristic peak is not closer than at least twice the value of FWHM, and the two adjacent peaks do not contribute into intensity of each other significantly. Unfortunately, energies of the peaks of different elements may have very close values. As a result, overlapping of the peaks creates a serious problem for identifying a real position and intensity of each of them directly using the functions of ADMCA software. This situation is illustrated in Fig. 5. Peak 1 belongs to K_α peak of an element with Z_1. Its K_β peak is invisible being hidden under K_α peak of an element with $Z_2 = Z_1+1$. The position of K_β peak of the element Z_1 and the position of K_α peak of the element Z_2 may differ by several channels which is not visible in the spectrum.

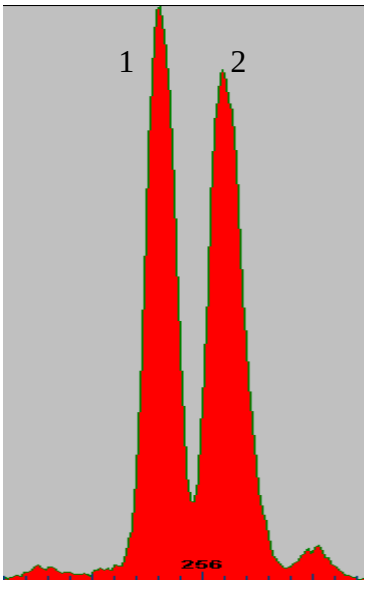

FIG. 5: Overlapping peaks of adjacent chemical elements.

To resolve this problem, the two methods can be applied either separately or together to confirm the result of each other. Both methods use relative intensity $R_{\beta\alpha}$ of K_β and K_α peaks that can be found in the Table 1-3 of the source [3] of APPENDIX D. For both methods you will calculate an intensity of a peak as an area under the peak curve, but not amplitude of the peak.
Following the first method, one restores the invisible K_β peak of the element Z_1, calculates the intensity (the area) of this peak, its position and amplitude, and subtracts the corresponding Gaussian peak from the total area under the peak 2 to obtain the improved position, shape and intensity (area) of the K_α peak of the element Z_2.

In the second method, which is less accurate, the K_β peak of the element Z_2 is used to calculate the intensity of the Kα peak of this element. In Fig. 5, the intensity of the peak 1 is greater than that of the peak 2; therefore, the first method would be more accurate for further calculation of exact values of intensities and quantitative analysis. The above described procedure may be performed with any fit (MATLAB, Python or other). However, a PC is sometimes unable to perform calculations with too many Gaussian peaks. It is a good idea to prepare the initial estimates as close to the real spectrum as possible.

Reference

1. Omer Sogut. Chinese Journal of Physics, **48**, 2 (2010).
2. Chen Ximeng et al. Journal of Radioanalytical and Nuclear Chemistry, **258**, 1 (2003).
3. X-Ray Data Booklet.. Lawrence Berkeley National Laboratory.
4. N. Kaya , E. Tırasoglu, G. Apaydın. Nuclear Instruments and Methods in Physics Research B **266,** 1043–1048 (2008)
5. Horst Ebel. X-Ray Tube Spectra, X-Ray Spectrometry, **28**, 255-266 (1999)
6. M. Van Gysel, P. Lemberge and P. Van Espen. X-Ray Spectrom. **32,** 139–147 (2003)

Experiment 1. Quantitative elemental analysis of coins.

First tested by **Paul Fox (PHY426, 2008)**
and **Siavash Aslanbeigi (PHY427, 2009)**

This experiment consists of two parts:

- obtaining and processing x-ray characteristic spectra of modern Canadian coins to calculate their composition, to compare the results to the coins' composition, given by Canadian Mint (see Table 1.1), and to evaluate the accuracy of the method;
- obtaining and processing x-ray characteristic spectra of ancient Chinese coins or a very old Canadian coin to calculate their chemical composition, which is initially unknown.

TABLE 1.1. COMPOSITION OF CANADIAN COINS
The following information is available from Canadian Mint
http://www.bcscta.ca/resources/hebden/chem/Coin%20Compositions.pdf

Valu	Years	Mass (g)	Composition
1¢	1920-41	3.24	95.5% Cu, 3.0% Sn, 1.5% Zn
	1942-77	3.24	98.0% Cu, 0.5% Sn, 1.5% Zn
	1978-79	3.24	98.0% Cu, 1.75% Sn, 0.25% Zn
	1980-81	2.8	98.0% Cu, 1.75% Sn, 0.25% Zn
	1982-96	2.5	98.0% Cu, 1.75% Sn, 0.25% Zn
	1997-99	2.25	98.4% Zn, 1.6% Cu plating
	2000-	2.35	94.0% steel, 4.5% Cu, 1.5% Ni, (*) (NOTE: Magnetic!)
5¢	1920-21	1.167	20% Cu, 80% Ag
	1922-42	4.54	99% Ni
	1942-43	4.54	88% Cu, 12% Zn
	1944-45	4.54	chrome plated steel
	1946-51	4.54	99.9% Ni
	1951-54	4.54	chrome plated steel
	1955-81	4.54	99.9% Ni
	1982-99	4.6	75% Cu, 25% Ni
	2000-	3.95	94.5% steel, 3.5% Cu, 2% Ni plating
10¢	1920-67	2.33	80.0% Ag; 20.0% Cu
	1968-77	2.07	99.9% Ni
	1978-99	2.07	99% Ni
	2000-	1.75	92% steel, 5.5% Cu, 2.5% Ni plating
25¢	1920-67	5.83	80.0% Ag; 7.5% Cu
	1967-68	5.05	50.0% Ag; 50.0% Cu
	1968-99	5.05	99.9% Ni
	2000-	4.4	94% steel, 3.8% Cu, 2.2% Ni plating
$1	1987-	7	91.5% Ni electroplated with 8.5% bronze plating
$2	1996-	7.3	outer ring = 99% Ni; inner core = 92% Cu, 2% Ni, 6% Al
(*) Note that some pennies in 2000-01 had copper-plated steel compositions, as evidenced by a small "P" under the Queen.			

Plating is the general name for surface-covering techniques in which a metal is deposited onto a conductive surface. Plating provides a surface of a metal with corrosion and abrasion resistance.

As you have already done the compulsory exercises for this experiment, you have a calibration function for energy vs. channel to calculate energy of any peak in the characteristic x-ray spectrum. Identification of characteristic peaks results in qualitative analysis of a sample.

Usually, coins consist of one or two main metals and a lot of impurities whose small amounts in the sample are called *the traces*. When the amount of an element in the sample is smaller or on the order of magnitude of the uncertainty in its determination, this component can be reported as *a trace element* without specific value for its amount. However, you can also find a different definition for the trace element with a specific upper level concentration in a sample. Using Table 1.1 and a set of coins available for this experiment in the laboratory select a couple of different coins that may be interesting to analyze. The main criteria for selection are:

- They should not be plated, otherwise you will see almost exclusively the spectrum of the metal, deposited on the surface of the coin.
- They should contain at least two metals.
- They should contain copper.
- The absorption edge of each component must have energy that satisfies specifications for our equipment, namely, the voltage across the x-ray tube and the range of energies available for analyzing with the spectrometer (see APPENDIX B).

Some important spectroscopic data for this experiment, can be found in APPENDIX D or on http://www.csrri.iit.edu/periodic-table.html and http://csrri.iit.edu/mucal.html .

1. QUANTITATIVE ANALYSIS OF CANADIAN COINS USING CALIBRATION WITH STANDARD SAMPLES

In this method, to obtain amount of a particular metal in a sample, you need to calibrate the vertical scale of a spectrum obtained from the MCA for “amount of an element” vs. “number of counts in characteristic peak”. The latter is called the *peak intensity*.

A procedure of calibration “amount vs. intensity” starts with analysis of a set of standard samples with known amount of all or just one component. You have a set of nine standard samples with the amount of Sn (tin) given in the Table 1.2.

TABLE 1.2. TYMETAL GA Series: Cu/Sn binary alloys which are used to prepare the basic calibration curve for Sn from 0% to 18%. Cu is the balance in all samples.

Standard	% Sn
GA1	2.31
GA2	3.95
GA3	5.78
GA4	8.25
GA5	9.96
GA6	12.27
GA7	13.94
GA8	16.18
GA9	18.10

We will consider that the amount of copper can be estimated as 100% - C_{Sn}. However, you will see the traces of other elements in the spectra and your records should show the entire composition of the sample at least qualitatively.

The standard alloys are in MP 245 by the setup. Using your results for the best gain, number of channels and time of acquisition, take spectra of all alloys from Table 1.2. Plot the composition of Cu vs. intensity of the K_α peak of copper. Create a similar calibration function for tin.

==========

Question 1. Do you expect a linear function for calibration? Why?

==========

a) Apply the Python or MATLAB fitter (or any other) to find a function of best fit for the calibration curves (http://www.physics.utoronto.ca/~phy326/python/index.htm#Fitting)
b) Take spectra of selected coins.
c) Find concentration of Cu (and Sn if applicable) using the calibration function.
d) Compare your results with the expected values from Table 1.1.
e) Evaluate the error in concentration of an element in this exercise; point out the main sources of uncertainties of the method [1, 2]; compare the experiment uncertainty with the difference between the measured and the expected values.
f) Select one more coin with plating and try to estimate the thickness of the plating using the data for attenuation coefficients from APPENDIX D and the data of Table 1.1.

2. ANALYSIS OF THE 19TH CENTURY CANADIAN COIN AND/OR 17th CENTURY CHINESE COINS

Request for the unique coins from the experiment supervisor.

Figure 1.1 shows a spectrum of a coin zoomed in for discovering the peaks of impurities.

Zooming is available from the ADMCA software (see Part I of the experiment) and should be used for preliminary estimate of the number of trace elements to consider in the analysis.

a) Acquire a spectrum of one of the coins with unknown composition.

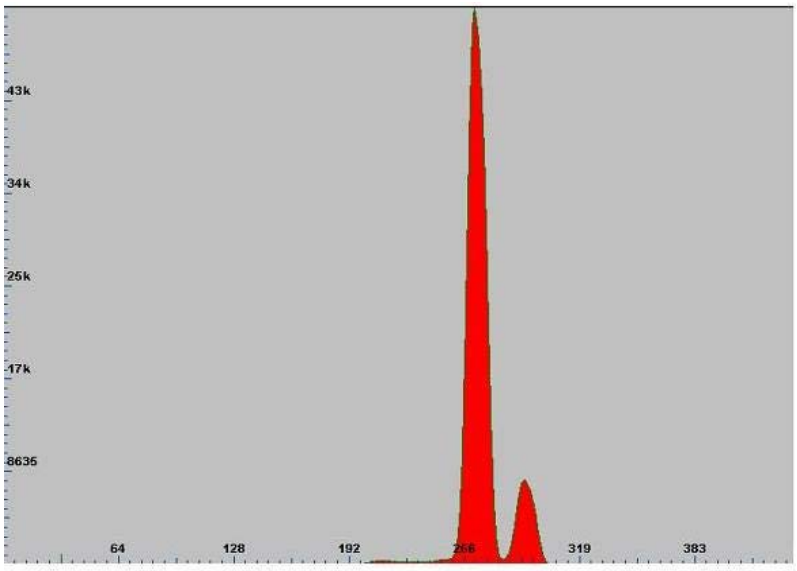

19th Century Canadian Coin 1

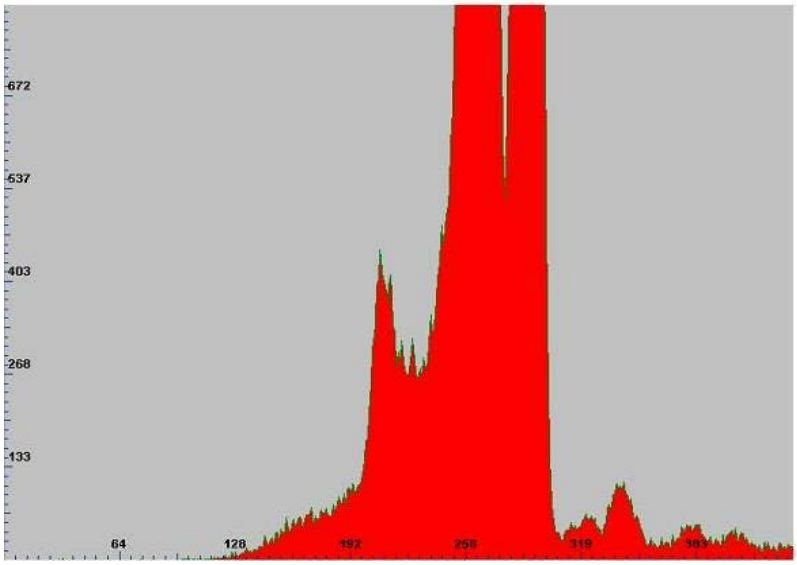

FIG. 1.1. X-ray spectrum of the 19th century Canadian coin

b) Determine whether the spectrum contains Cu or Sn.
c) Find the amount of copper as explained in the first exercise.
d) If tin has been discovered in the coin, find the amount of tin. Check for both Sn K-series and Sn L-series.
e) For other elements of the coin you can perform so-called semi-quantitative analysis, using additional simplification of Eq.14 of the Introduction and criteria of precision and accuracy in processing peaks with pretty low intensity [1, 2].

The usual method of simplification is interpreting a spectrum of the x-ray tube as a monochromatic spectrum, as if it consists of photons of same energy, or monoenergetic photons. This simplifies Eq. 14 to

$$N_i = \left(\frac{1}{\sqrt{2}}G\right)\cdot\left[\varepsilon_i \omega_i p_{tr,i}\left(1-\frac{1}{r_i}\right)\right]\frac{\tau_{1i}C_i}{\sum \mu_{1j}C_j + \sum \mu_{ij}C_j}\cdot N_1 \qquad (1.1)$$

where absorption and attenuation coefficients of the primary radiation are related to the energy of Ag K_α line and N_1 is the intensity of the Ag K_α peak in our apparatus. N_1 in the Eq.1.1 is a constant coefficient in the equation for any element of the target. The ratio of the Eq.1.1, written for two elements with one of them Cu (or Sn), could give a good estimate for any unknown component of the coin even in absence of its standard sample. Test this method if the unknown component of the coin you are studying has a K_α or L_α peak energy close to 8.0 keV.

As it is well known, any filter between a source and a target decreases flux. However, there is a thin Al filter inserted into our device between the source and the sample.

==========

Question 2. Make a guess on the purpose of using the Al filter in the x-ray tube in this experiment. You may study the x-ray source spectrum with and without the filter here http://amptek.com/products/mini-x-ray-tube/#6 .

==========

REFERENCES

[1] R.Redus et al. *Benefits of improved resolution for edxrf* . Advances in X-Ray Analysis, **52**, (2008)
[2] Tomoya arai. *Analytical precision and accuracy in x-ray fluorescence analysis*. The Rigaku Journal **21**, 2 (2004), 26–38.
[3] L. Avaldi, L.Confalonieri, M. Milazzo, E. Paltrinieri, R. Testi, Quantitative results of xrf analysis of ancient coins by monochromatic x-ray excitation, Archoeometry **26**, 1 (1984).
[4] S.M. Simabuco, V.F. Nascimento Filho. Quantitative analysis by energy dispersive X-ray fluorescence by the transmission method applied to geological samples, Scientia Agricola, Piracicaba **51,** 2 (1994).

Experiment 2. Study of Si PIN detector in x-ray fluorescence spectrometer

First tested by **Owen Melville (PHY 427, 2008)**
and **Ray Xu (PHY 327, 2009)**

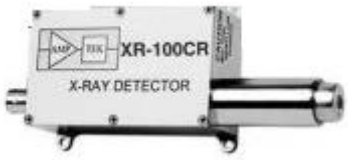

XR-100CR
2-stage cooler
13 mm^2 / 500 μm
1.0 mil (25 μm) Be
174 - 200 eV (according to the Manufacturer)
P/B Ratio: 550/1 (4000/1 with external collimator)
*Peaking Time is approximately 2.4x shaping time.
**The Peak to Background (P/B) Ratio is the ratio of the counts at the 5.9 keV peak to the counts at about 2 keV.

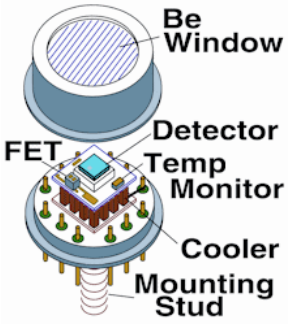

FIG.2.1: Si PIN detector unit. FET is a field-effect transistor

INTRODUCTION

Theory of Operation

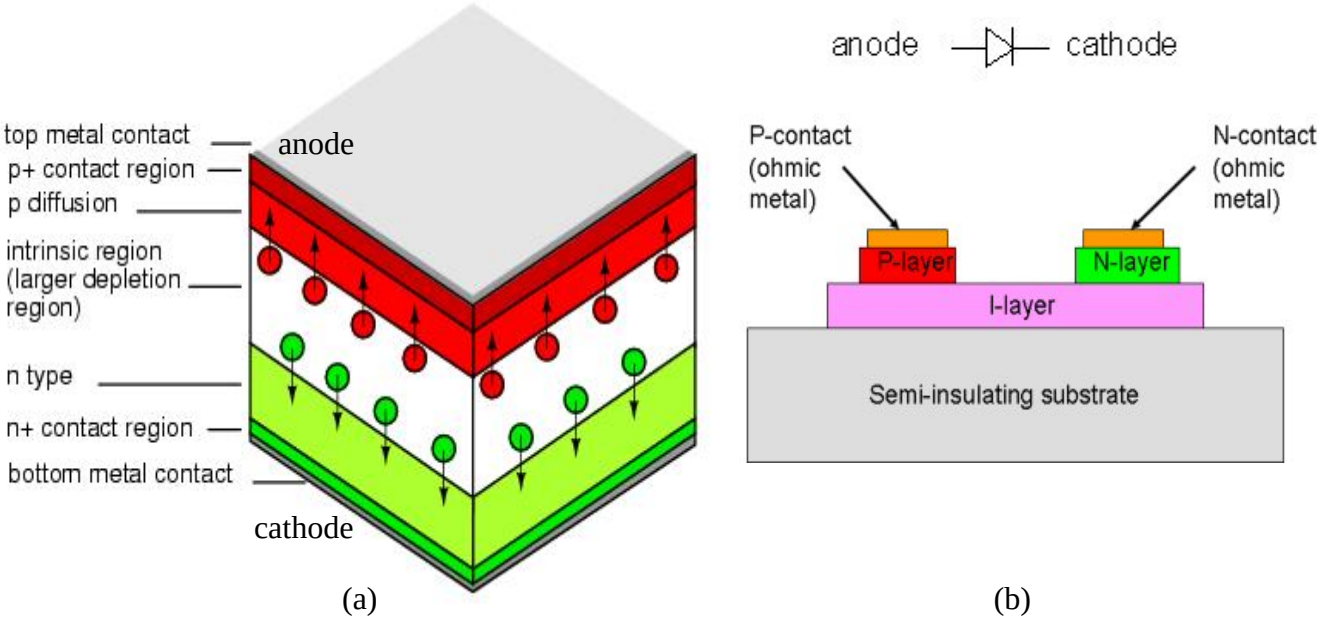

(a) (b)

FIG.2.2: PIN diode: (a) – structure of regions;
(b) – spatial arrangement of the PIN diode elements

X-rays interact with silicon atoms to create an average of one electron/hole pair for every 3.62 eV of energy lost in the silicon. Depending on the energy of the incoming radiation, this loss is dominated by either the Photoelectric Effect or Compton scattering. The probability or efficiency of the detector to "stop" an x-ray and create electron/hole pairs increases with the thickness of the silicon (see efficiency curves).

In order to facilitate the electron/hole collection process, a 100-200 volt bias voltage is applied across the silicon depending on the detector thickness. This voltage is too high for operation at room temperature, as it will cause excessive leakage, and eventually breakdown. Since the detector in the XR-100CR is cooled, the leakage current is reduced considerably, thus permitting the high bias voltage. This higher voltage decreases the capacitance of the detector, which lowers system noise.

The thermoelectric cooler cools both the silicon detector and the input FET transistor to the charge sensitive preamplifier. Cooling the FET reduces its leakage current and increases the transconductance, both of which reduce the electronic noise of the system.

Since optical reset is not practical when the detector is a photodiode, the XR-100CR incorporates a novel feedback method for the reset to the charge sensitive preamplifier. The reset transistor, which is typically used in most other systems, has been eliminated. Instead, the reset is done through the high voltage connection to the detector by injecting a precise charge pulse through the detector capacitance to the input FET. This method eliminates the noise contribution of the reset transistor and further improves the energy resolution of the system.

A temperature monitor diode chip is mounted on the cooled substrate to provide a direct reading of the temperature of the internal components, which will vary with room temperature. Below -20 °C, the performance of the XR-100CR will not change with a temperature variation of a few degrees. Hence, closed loop temperature control is not necessary when using the XR-100CR at normal room temperature. For OEM applications or hand held XRF instrumentation a closed loop temperature control is recommended. The Active Temperature Control is optional in the PX2CR and standard in the PX4.

Thermoelectric cooling

How do thermoelectric coolers (TECs) work?

A **Peltier cooler**/heater or thermoelectric heat pump is a solid-state active heat pump which transfers heat from one side of the device to the other. Peltier cooling is also called *thermo-electric cooling* (TEC). If a power source is provided, the thermoelectric device may act as a cooler, as in the figure to the left below. This is the Peltier effect. Electrons in the n-type element will move opposite the direction of current and holes in the p-type element will move in the direction of current, both removing heat from one side of the device.

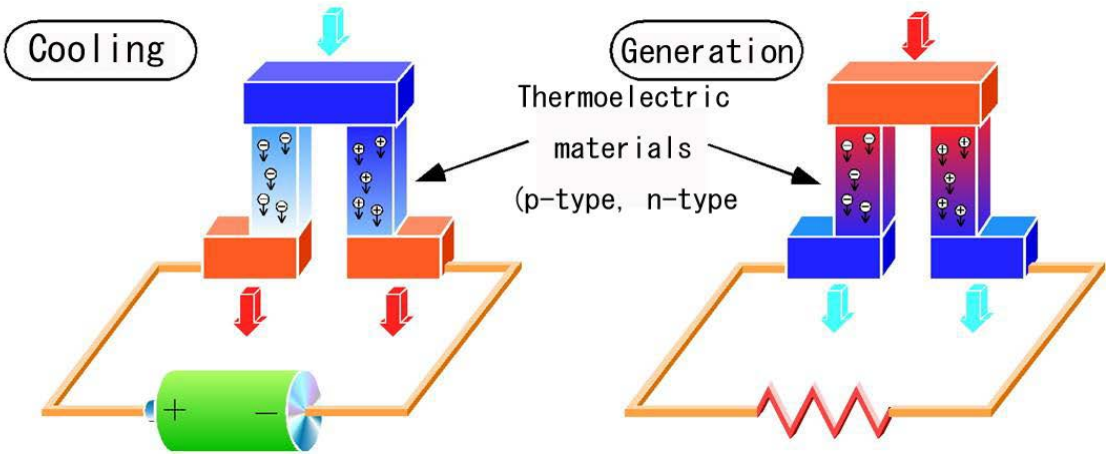

FIG.2.3: Thermoelectric effects of cooling (Peltier Effect) and generating power

http://www.peltier-info.com/animation1.gif - animation of a Peltier cooler functioning.

Thermoelectric coolers are solid state heat pumps that operate on the Peltier effect, the theory that there is a heating or cooling effect when electric current passes through two conductors. A voltage applied to the free ends of two dissimilar materials creates a temperature difference. With this temperature difference, Peltier cooling will cause heat to move from one end to the other. A typical thermoelectric cooler will consist of an array of p- and n- type semiconductor elements that act as the two dissimilar conductors. The array of elements is soldered between two ceramic plates, electrically in series and thermally in parallel. As a dc current passes through one or more pairs of elements from n- to p-, there is a decrease in temperature at the junction ("cold side") resulting in the absorption of heat from the environment. The heat is carried through the cooler by electron transport and released on the opposite ("hot") side as the electrons move from a high to low energy state. The heat pumping capacity of a cooler is proportional to the current and the number of pairs of n- and p- type elements (or couples).

APPENDIX C gives the answers to the most frequently asked questions about thermoelectric cooling.

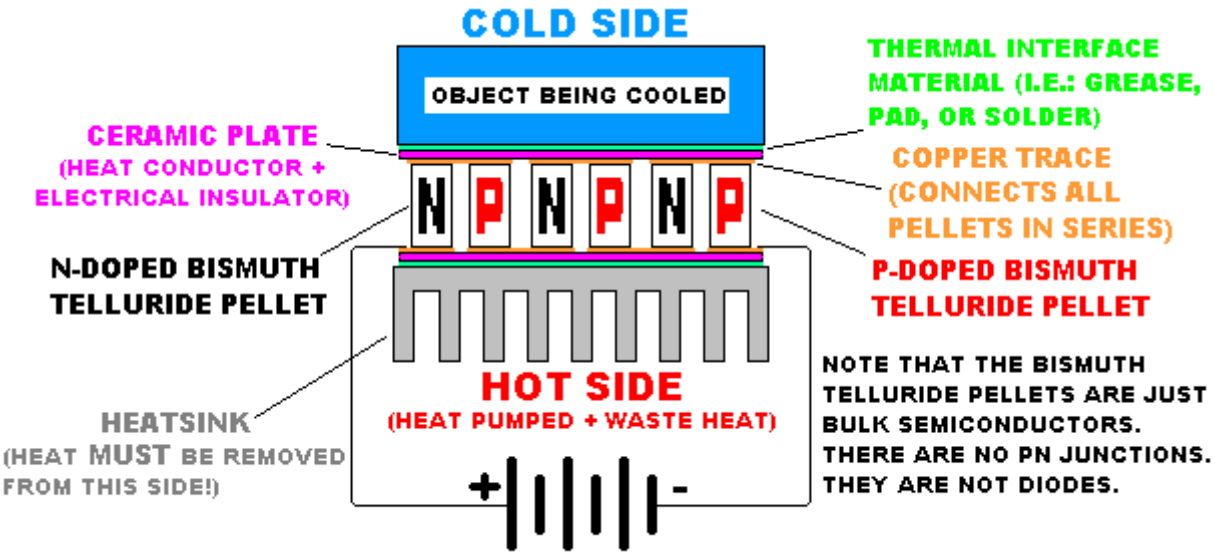

FIG.2.4: More detailed scheme of the Peltier element functioning

The main properties of a detector are:

I. Efficiency
II. Resolution
III. Sensitivity

I. EFFICIENCY

Figure 2.5 combines the effects of transmission through the Beryllium window (including the protective coating), and interaction in the silicon detector. The low energy portion of the curves is dominated by the thickness of the Beryllium window, while the high energy portion is dominated by the thickness of the active depth of the Si detector. Depending on the window chosen, 90% of the incident photons reach the detector at energies ranging from 2 to 3 keV. Depending on the detector chosen, 90% of the photons are detected at energies up to 9 to 12 keV.

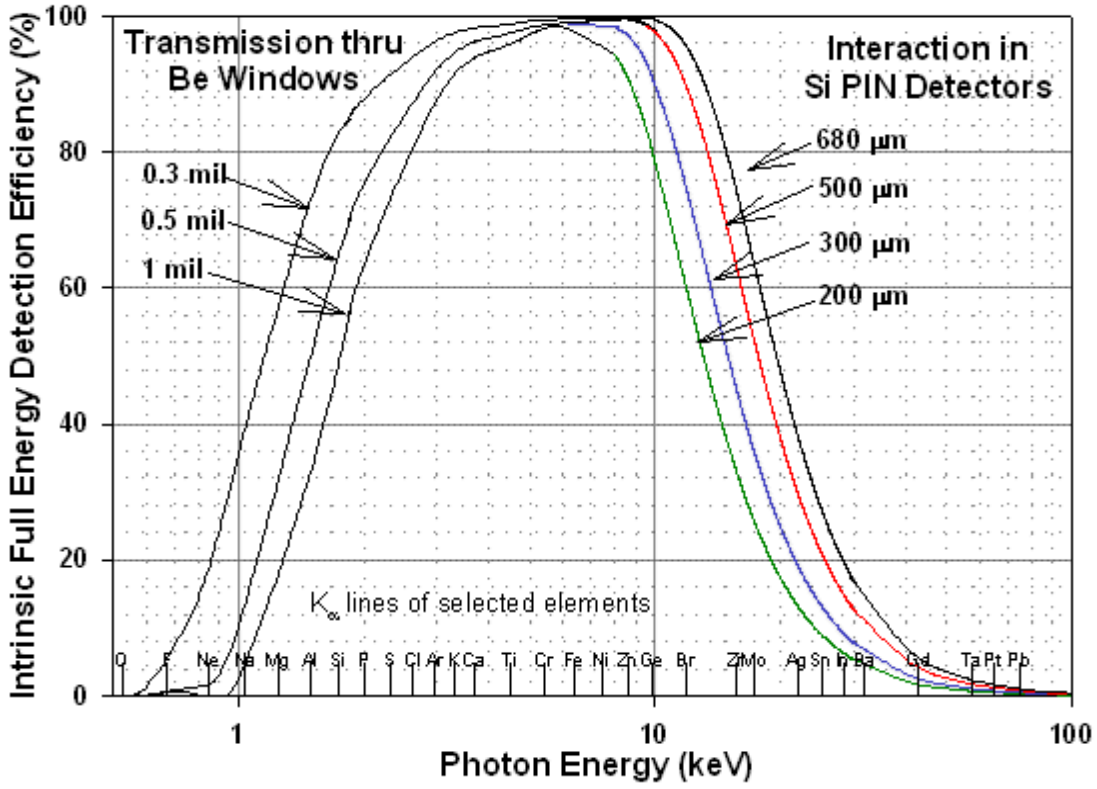

FIG. 2.5. The intrinsic full energy detection efficiency for Si-PIN detectors. This efficiency corresponds to the probability that an X-ray will enter the front of the detector and deposit all of its energy inside the detector via the photoelectric effect.

The efficiency vs. energy table is given in
http://amptek.com/products/xr-100cr-si-pin-x-ray-detector/#6

Set the number of channels to 1024. Find the efficiency of your detector using the samples of pure metals. Find the detector response function for different gain settings. Conclude on the choice of gain setting for obtaining the best efficiency for different ranges of spectrum. Find a function to fit your results and graph the function.
How does your function of efficiency correspond to the data in Fig. 2.5?

II. RESOLUTION

Theoretical Resolution as a Function of Energy

$$eV_{fwhm} \ @ \ E_x = \left[(eV_{fwhm} \ @ \ 5.9 \ keV)^2 - 120^2 + 2440 \ E_x \right]^{\frac{1}{2}} \qquad (2.1)$$
$$\text{Where} \quad E_x = Energy \ in \ keV$$

In an experiment, the resolution is understood as a quantity that reflects whether two adjacent peaks are resolved, or that the two adjacent peaks are treated as two different peaks in spite of their overlapping.

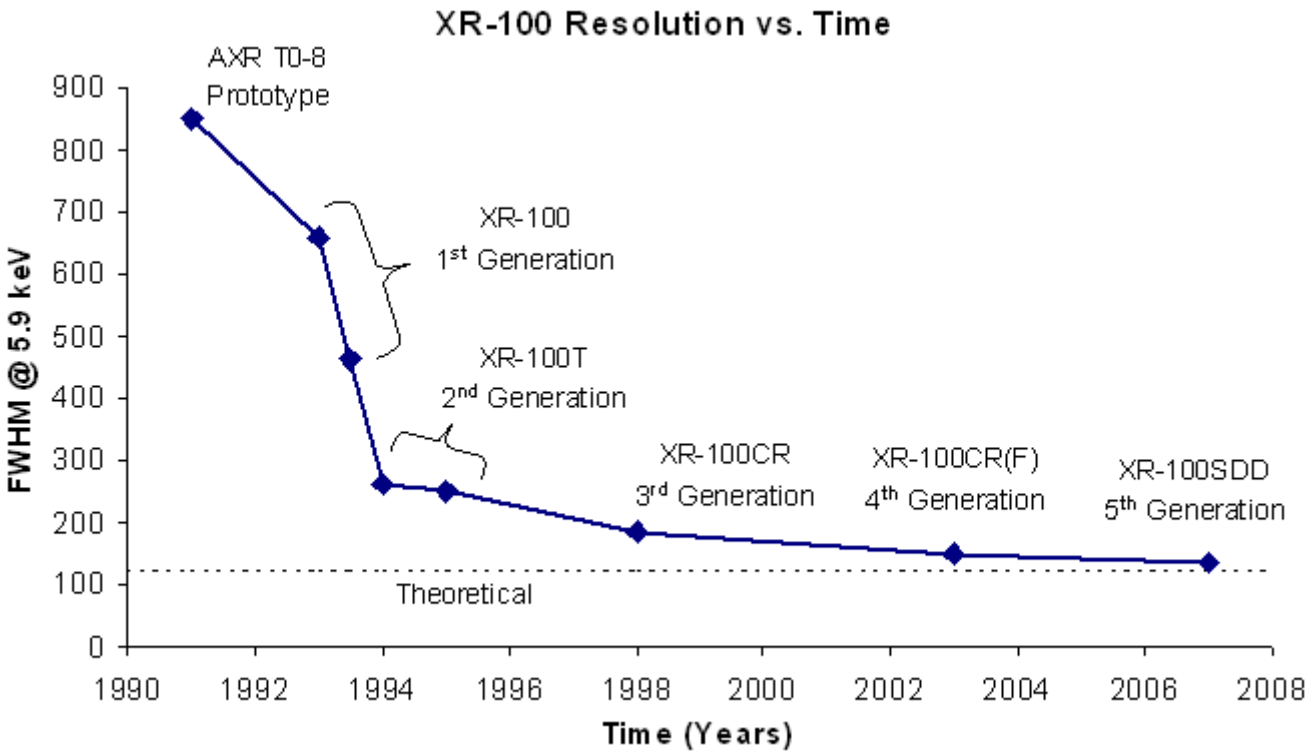

FIG.2.6: History of XR-100 Resolution

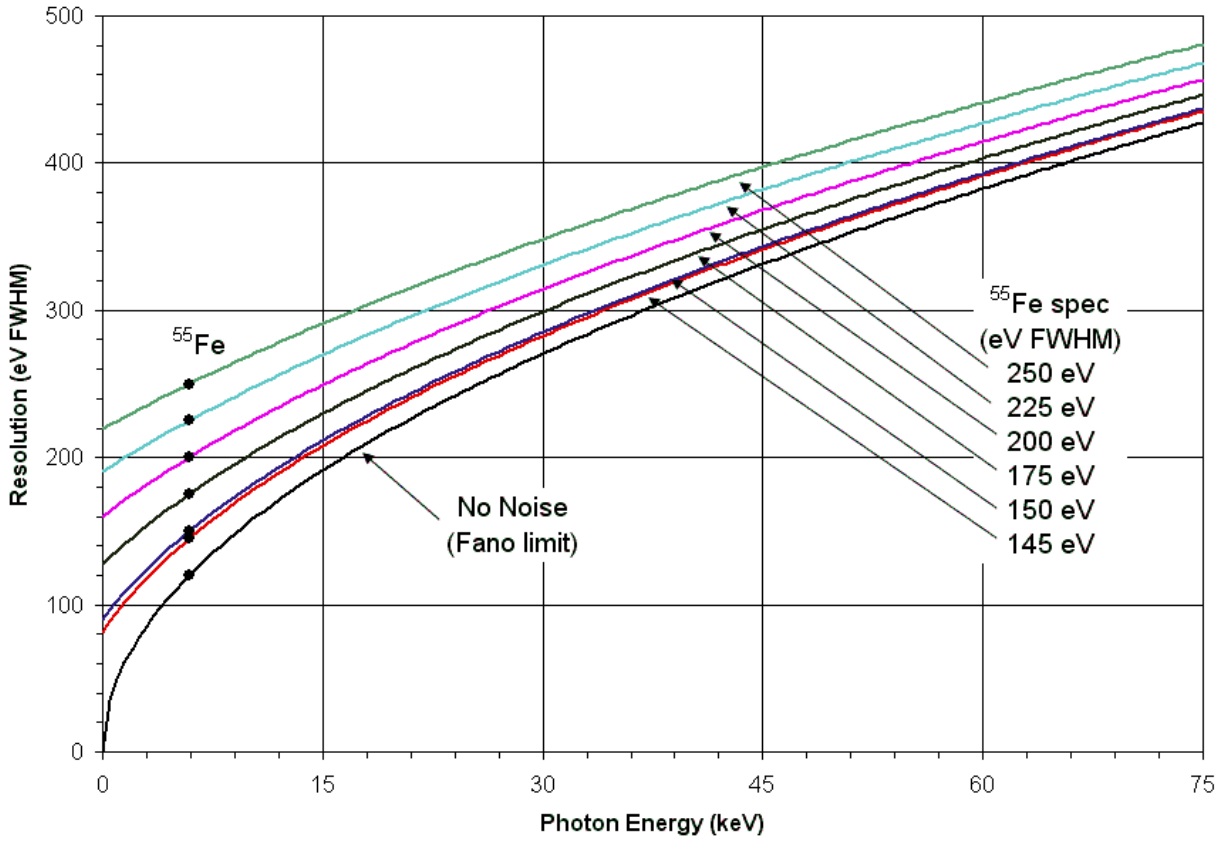

FIG.2.7: Resolution as a function of energy for various detector resolutions. For example, a detector with a ^{55}Fe resolution of 145 eV FWHM will follow the red curve.

TABLE 2.1.
Resolution at Common Characteristic X-ray Energies

	Energy	Total Resolution (eV FWHM)					
Electronic Noise		81	90	127	160	190	219
Al K_α	1.49	101	108	141	171	200	227
S K_α	2.31	111	117	148	177	205	232
Ag L_α	2.98	118	124	153	181	209	235
Cr K_α	5.41	141	146	172	197	222	248
^{55}Fe	5.89	**145**	**150**	**175**	**200**	**225**	**250**
Cu K_α	8.05	162	167	189	213	236	260
Au L_α	9.71	174	178	200	222	245	268
Hg L_α	9.99	176	180	202	224	246	269
Pb L_α	10.55	180	184	205	227	249	272
U L_α	13.61	200	203	222	243	264	285
Mo K_α	17.48	222	225	243	261	281	301
Ag K_α	22.16	246	249	265	282	301	320
Sn K_α	25.27	261	264	279	295	313	331

Example: Find the ^{55}Fe row in the above table and locate the resolution of the detector (bold). The column with that resolution lists the resolutions of that detector for these common energies.

The resolution of a detector must be improved by all means to improve the accuracy of EDXRF analysis [1].

Set the number of channels to 1024. Using radioactive source ^{109}Cd and samples of pure metals, find the function of resolution of your detector vs. energy of a peak for different gains. How close is your function to formula Eq.2.1? What gain would you recommend for experiments with the given samples? Repeat the experiment with 512, 2048, and 4096 channels for the full scale. Compare resolution of the spectrometer for different scales.

III. SENSITIVITY (PEAK TO BACKGROUND RATIO)

Use of Collimators

X-ray events that are produced near the edges of a detector may result into partial charge collection. Hence, a typical "tail" is observed at the low energy side of an energy peak. This "tail" is often called the "Background".
In the case of the ^{55}Fe, the ratio of the counts at the 5.9 keV peak to the counts at about 2 keV is called the "Peak to Background Ratio" (P/B).
The XR-100CR with a 7 mm^2 uncollimated detector exhibits a P/B = 260. However, the same detector with an external Aluminum collimator having a 2 mm diameter hole has a P/B = 3150. Most of Amptek's detectors contain internal collimators to improve spectral quality. X-rays interacting near the edges of the active volume of the detector may produce small pulses due to partial charge collection. These pulses result in artifacts in the spectrum which, for some applications, obscure the signal of interest. The internal collimator restricts X-rays to the active volume, where clean signals are produced. Depending on the type of detector, collimators can

- improve peak to background (P/B)
- eliminate edge effects
- eliminate false peaks

The use of a collimator increases the signal to noise ratio of X-ray events that fall on the low energy tails of higher peaks, and thus increasing the counting statistics in observing such events.

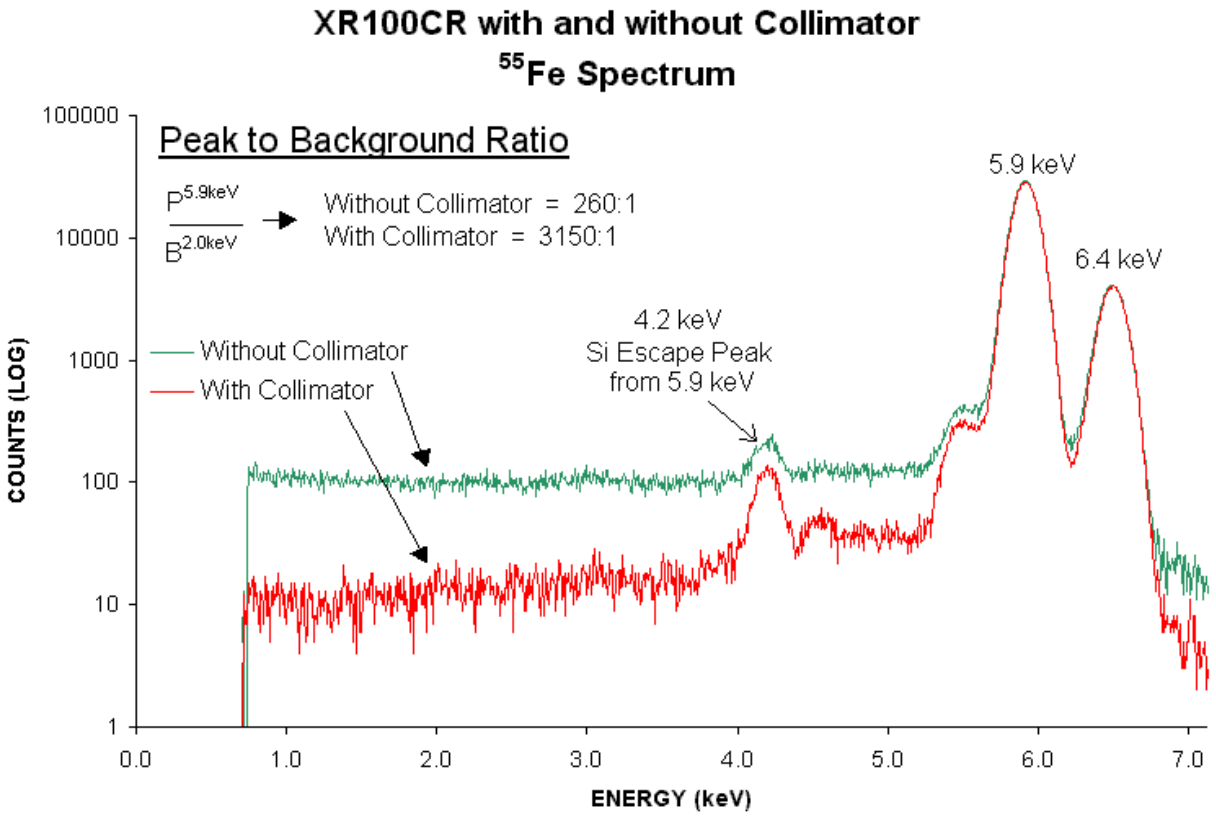

FIG.2.8: Effect of an external collimator to the P/B ratio in the spectrum of ^{55}Fe.

Rise Time Discriminator (RTD) for the 7 mm^2/300 µm or 13 mm^2/300 µm Detectors

The 13 mm^2/300 µm detectors are partially depleted. From the total thickness of 300 µm, approximately the front 200 µm are totally depleted. The remaining 100 µm near the back contact are partially depleted. Electron-hole pairs created by X-Rays which interact with the silicon near the back contact of the undepleted detector are collected more slowly than normal events. These events can result in smaller than normal charge collection and may increase the peak to background ratio (P/B) in the energy spectrum. In partially depleted detectors these events produce secondary peaks that need to be removed. To remove the secondary peaks, both the PX2CR and the PX4 incorporate a Rise Time Discrimination circuit (RTD) which prevents these pulses from being counted by the MCA. See figure 8. All spectra shown in this specification were taken using RTD.

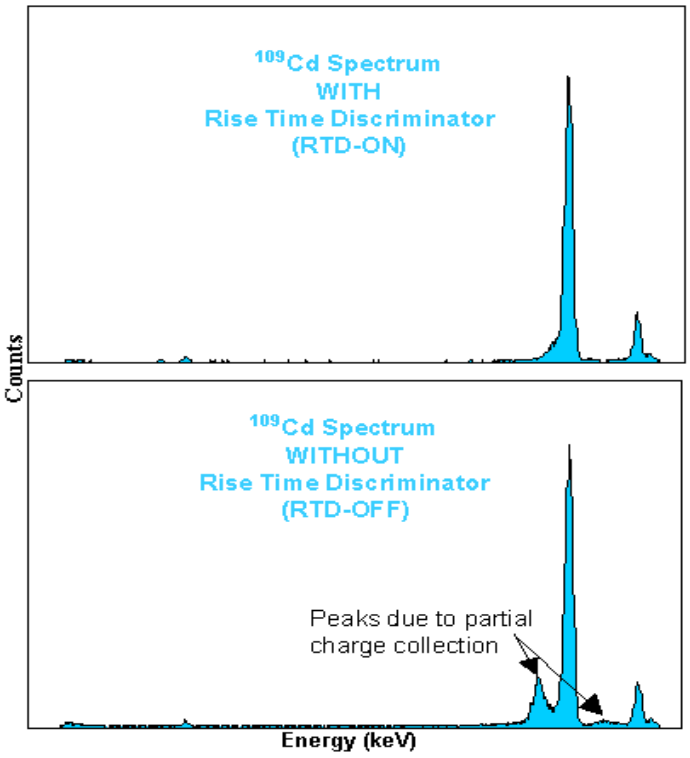

FIG.2.9: Spectrum improvement with a Rise Time Discriminator

Formulate the procedure to determine the sensitivity of the detector.

The manufacturer guide for the XR100 Si-PIN detector can be found on the web site: http://www.amptek.com/xr100cr.html

Compare the results of your measurements for efficiency and resolution with the values provided by the manufacturer.

Questions

1. What is the reason to use a Be-window in the x-ray tube and in the detector?
2. Why the detector is called PIN?
3. Sketch a structure of the Si PIN device, explain its functioning and main advantages compared to the p-n junction diode.
4. Why is it important to maintain low temperature for the semiconductor detector in a spectrometer? During the experiment discussion with a supervisor you will be asked to explain the Peltier Effect used for the detector cooling.
5. What advantages has the Peltier cooler compared to the liquid nitrogen cooling system for this experiment?
6. What is the efficiency of your detector at 5 keV and at 22 keV? Are they different? Why?
7. What is the resolution of your detector at 5 keV and at 22 keV? Are they different? Why?

References

1. R.Redus et al. *Benefits of improved resolution for edxrf* . Advances in X-Ray Analysis, **52**, (2008)

Experiment 3. Secondary x-ray fluorescence excitation and matrix effects in alloys.

First tested by **Siavash Aslanbeigi (PHY427, 2009)**
and **Isaak Pratt (PHY424, 2010)**

INTRODUCTION

In this experiment, you will investigate secondary excitation of x-ray fluorescence in atoms of one of the components of a sample induced by characteristic x-rays of the other elements of the sample. As a result, intensity of a characteristic peak of one of the components of the sample is formed by two contributions: the photons, induced by primary radiation of the x-ray tube, and the photons, induced by characteristic x-ray radiation of the other components of the sample. The intensity of the characteristic peak depends not only on the amount of the element and the amounts of the other elements for account for absorption and secondary enhancement, but also on how close the energy of characteristic peaks of all elements are to the absorption edge of the analyte (the chemical element being analyzed). Such inter-element interactions inside one sample are called *matrix effects*.

1. QUANTITATIVE ANALYSIS OF A BINARY ALLOY WITHOUT CONSIDERING SECONDARY ENHANCEMENT

You will study the matrix effects in a Fe-Ni alloy with concentration of nickel C_{Ni} = 83%. This sample is expected to show a significant difference in the results of analysis with and without corrections to the secondary enhancement of the Fe K-series.

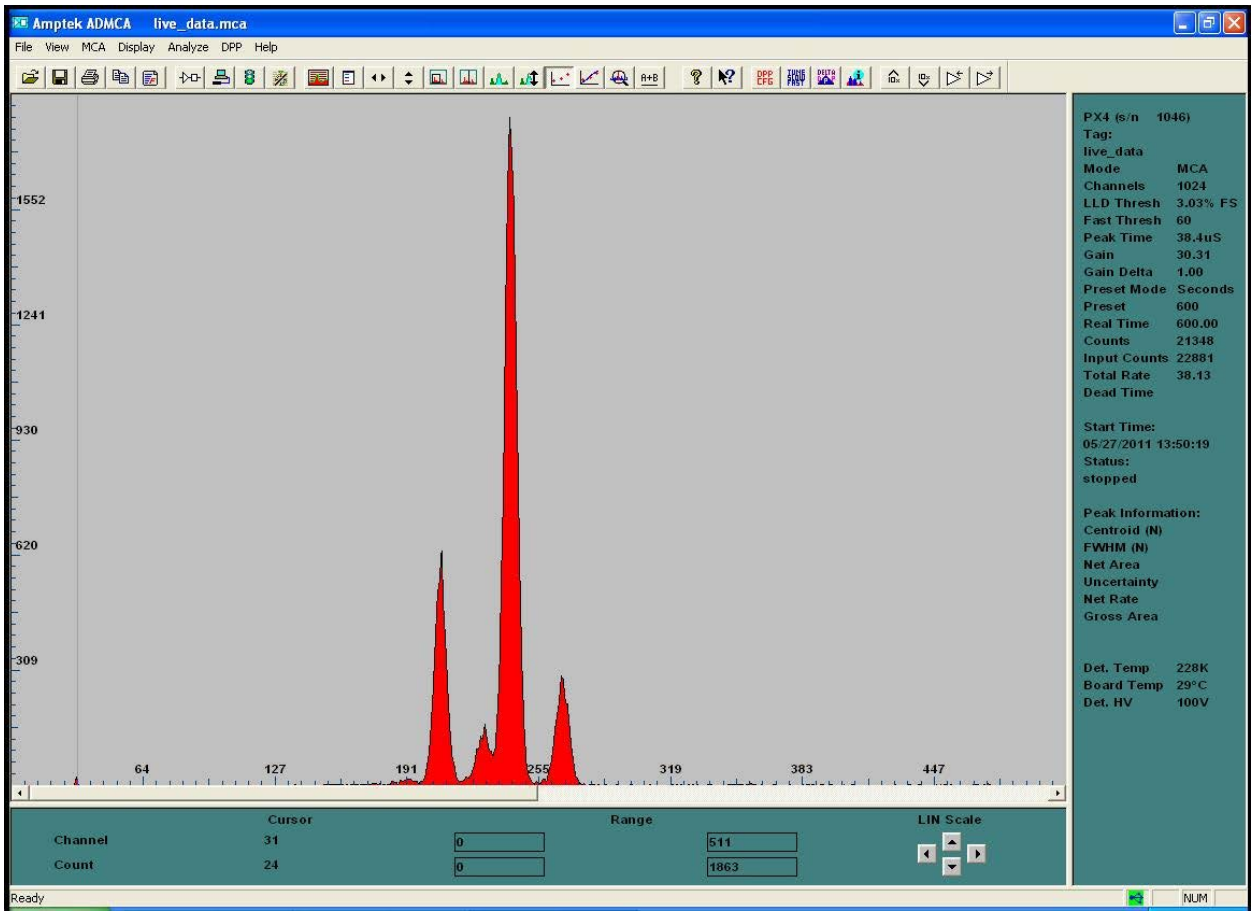

FIG.3.1. The Fe-Ni alloy spectrum, obtained in May 2011. The settings are shown in the green band to the right of the spectrum.

Periodic table with all necessary constants for quantitative analysis with energy-dispersive XRF method can be found in [5] of the APPENDIX D: http://www.csrri.iit.edu/periodic-table.html

Figure 3.1 shows a spectrum of the binary alloy Fe-Ni with given nickel concentration of 83%. For your experiment, you can try the other settings for the MCA to improve resolution. However, regardless the settings, the problem of peaks' overlapping will exist. The methods to resolve overlapping peaks are explained in the Introduction to Part II of the experiment.

The relative intensities of Fe K_α and Ni K_α either taken as areas under the peaks or estimated with the peaks amplitudes in Fig. 3.1 give an approximate ratio of iron and nickel concentration as 1:3 instead of real 1:5 (17% of Fe and 83% of Ni). For iron component, the difference is about 1.5 times! The only source of the discrepancy is neglecting the matrix effects of absorption and secondary enhancement.

For the main goal of this exercise, your determination of the characteristic peak intensity must be as precise as possible. This problem looks unresolvable since it is impossible to find the proper function $N_1(E)$ in the Eq.14. However, the manufacturer of the x-ray tube introduced a piece of equipment that gives a reasonably accurate solution: there is a thin Al filter inserted into our device between the source and the sample. Figure 3.2 gives an idea of the role of the filter:

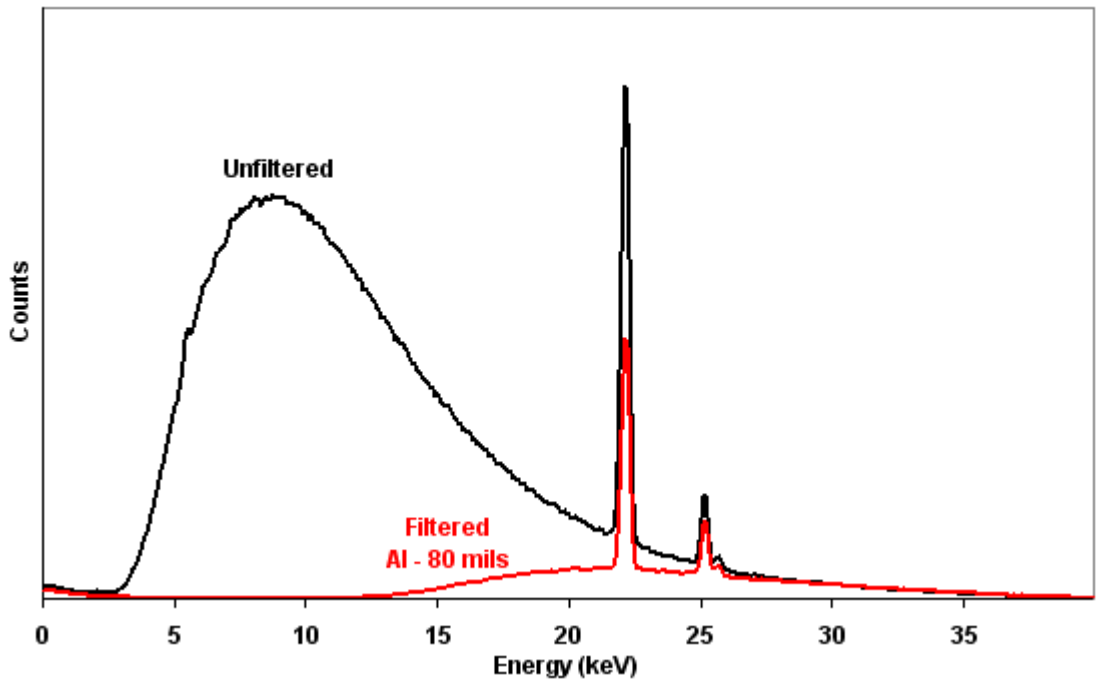

FIG. 3.2: MiniX-Ag output spectrum at 40 keV with and without 2-mm aluminum filter http://amptek.com/products/mini-x-ray-tube/#6 .

The usual method of simplification of Eq.14 is interpreting a spectrum of the x-ray tube as a monochromatic spectrum, as if it consists of photons of same energy, or monoenergetic photons. With aluminum filter inserted, we can consider the primary source spectrum being a spectrum of Ag K-series with a very good accuracy. This simplifies Eq. 14 to

$$N_{i1} = \left(\frac{1}{\sqrt{2}}G\right)\cdot\left[\varepsilon_i \omega_i p_{tr,i}\left(1-\frac{1}{r_i}\right)\right]\frac{\tau_{1i}C_i}{\sum \mu_{1j}C_j + \sum \mu_{ij}C_j}\cdot N_1 \qquad (3.1)$$

where absorption and attenuation coefficients of the primary radiation are related to the energy of AgK_α line and N_1 is the intensity of the AgK_α radiation of the x-ray tube in our apparatus. N_1 in the Eq.3.1 is a constant coefficient in the equation for both Fe and Ni intensities. The ratio of the Eq.3.1, written for two elements, could give a good estimate for the relative intensities of the components of the alloy and been re-organized, the relative concentration of the elements. On the other hand, we will assume the alloys consisting of just two elements for simplicity, so the sum of their concentrations is 100%.

1. You have pure Fe and pure Ni samples and a number of alloys with these two metals.
2. Choose the best settings for the MCA to take spectra of the given Fe, Ni and Fe-Ni samples.
3. Using the ROI function of the MCA and varying the peak width, obtain the most accurate values for intensities and positions for four peaks in the region of interest in each sample. The positions can be calculated basing on your calibration, made in Part I of the experiment.
4. Save the data in a *.txt file and after some modification of the file, enter it into MATLAB to get more accurate results for intensities of the four peaks. A good option is to use http://www.physics.utoronto.ca/~phy326/python/index.htm#Fitting – a web page on the Advanced Physics Laboratory web site with prepared Python codes. For quantitative analysis you need just two intensities: for K_α peaks of iron and nickel. However, due to the overlapping of the adjacent peaks, you have to accurately calculate the intensity of four peaks, assuming that their position is a known quantity and their shape is a Gaussian curve. To *estimate* standard deviation of the Gaussian peaks, it is possible to take the half of the value of FWHM (see the Glossary in Part I) considering it to be same for the four peaks. Actually, due to properties of the detector, the FWHM steadily increases with the increase of the energy of a peak, but this change is negligible for so closely located peaks as the peaks of Fe and Ni K-series.
5. It is reasonable to first calculate the ratio of iron and nickel concentrations C_{Fe} / C_{Ni} ignoring matrix effects of secondary enhancement. Ref.[3, 4,5] of APPENDIX D are the most convenient sources of necessary data for this exercise. Also see Table 3.1 below. For Ag K_α, the coefficient of absorption in iron is τ_{AgFe} = 17.83 g/cm^2; and the coefficient of absorption in nickel is τ_{AgNi} = 23.59 g/cm^2. The attenuation coefficients must be calculated as given by Eq.5. With unknown concentrations of two components of the alloy, the other simplification may be taken: instead of attenuation coefficients in a matrix, you will have to use the attenuation coefficients in pure nickel, as in practice we usually can preliminary estimate which component has the greatest concentration. Otherwise the calculation procedure will include a number of iterations. Combine the result for C_{Fe} / C_{Ni} with the equation C_{Fe} + C_{Ni} = 100 and calculate concentrations of iron and nickel in the alloy taking into consideration the matrix effect of attenuation and ignoring the secondary enhancement. Detector efficiency for Fe and Ni peaks can be taken as 1 (see Fig. 2.5 on p.19).

2. QUANTITATIVE ANALYSIS OF A BINARY ALLOY WITH CONSIDERING MATRIX EFFECT OF SECONDARY ENHANCEMENT

In the given alloy, the matrix effects are expected to be significant. The table in APPENDIX A gives energy of the Ni K_α peak as 7.48 keV. The table in APPENDIX B gives energy of excitation of the K-level of the iron atom as 7.11 keV. Thus, energy of the photons emitted by the atoms of nickel is slightly higher than the excitation energy of the K-level of the atoms of iron.

Figure 3.3 gives the coefficient of absorption for Fe as a function of energy of the incident photons. The jump in absorption at the energy of 7.11 keV means that the probability of excitation of atoms of iron drastically rises at this energy, which is very close to the energy of Ni

K_α peak. In terms of quantum mechanics same conclusion can be formulated as the jump in probability of absorption, or the jump in the cross section of the absorption. The coefficient of absorption has a dimension of a specific cross section, which is cm^2/g. At the absorption jump, the role of the secondary enhancement becomes significant.

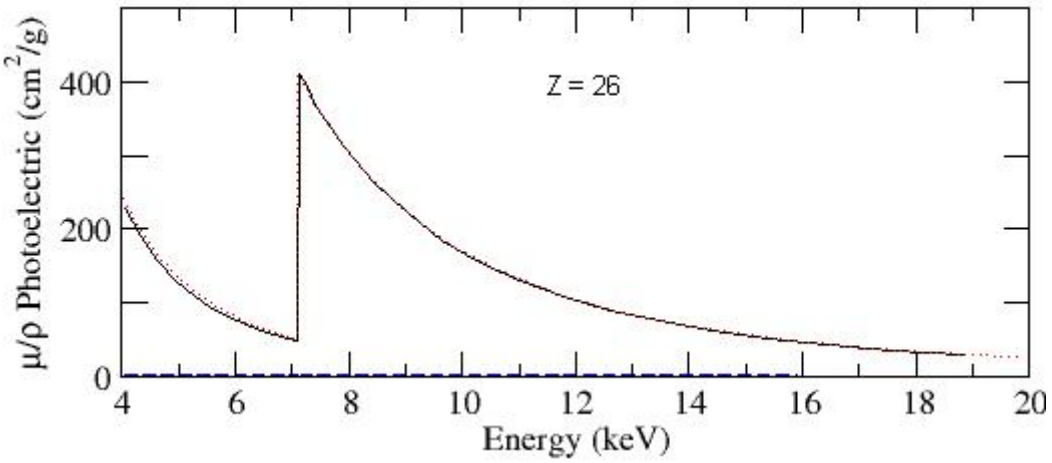

FIG. 3.3. Mass-absorption coefficient in iron as a function of energy of the absorbed photons.

The formula for calculation of the concentration of components in the sample where the matrix effect of secondary enhancement must be accounted for, is given in Eq. 9 of the reference source [1] (see also a hard copy of the article attached to the experiment handout). In our handout notation, the formula looks as follows:

$$N_i = N_{i1}(1+\gamma_{ji}); \quad \gamma_{ji} = \frac{1}{2}\omega_j p_{tr,j}\left(1-\frac{1}{r_j}\right)\frac{\tau_{1j}\tau_{ji}C_j}{\tau_{1i}}\left\{\frac{1}{\sqrt{2}\mu_{1t}}\ln\left(\frac{\sqrt{2}\mu_{1t}}{\mu_{jt}}+1\right)+\frac{1}{\sqrt{2}\mu_{it}}\ln\left(\frac{\sqrt{2}\mu_{it}}{\mu_{jt}}+1\right)\right\} \tag{3.2}$$

where N_{i1} is given by (3.1); $\sqrt{2} = \frac{1}{\cos\varphi} = \frac{1}{\cos\psi} = \frac{1}{\cos 45^o}$; *i* identifies quantities of iron; *j* identifies quantities of nickel; 1 in a subscript refers to Ag K_α; and μ_{1t}, μ_{it} and μ_{jt} should be calculated according to Eq.5 of Introduction to the Part II. Equation 3.1 for N_{i1} gives the expected peak intensity of iron K_α in absence of the secondary enhancement by K-series x-rays of nickel. You have actually used it in the first exercise of this experiment. The quantity γ_{ji} gives a relative contribution of the secondary enhancement effect into the total intensity of the K_α peak of iron. Equation 3.2 is valid for a binary alloy and must be modified for more complicated composition as $N_i = N_{i1}\,(1 + \Sigma\gamma_{ji})$.

Equations 3.1 and 3.2 cannot be used directly to calculate the components concentration, but will demand an iteration procedure, because the values of attenuation coefficients and absorption coefficients contain the unknown concentration. You are expected to apply your skills in programming with Python and/or Matlab to compute.

- Calculate the experiment uncertainty of each value of concentration.
- Compare your result with the result of the Part I of this exercise taking into account the uncertainties for both values. Conclude on the precision and accuracy of the results.
- Take spectra of the Fe-Ni alloy with unknown composition and calculate the amount of iron and nickel in the sample.

REFERENCE

[1] L. Avaldi et al. *Quantitative results of XRF analysis of ancient coins by monochromatic x-ray excitation.* Archaeometry **26**, 1 (1984).

TABLE 3.1. Useful constants

	ω	p_{tr}	r	E_K, keV	$E_{K\alpha}$, keV	$\mu_{\mathrm{Fe,\,i}}$, cm^2/g	$\mu_{\mathrm{Ni,i}}$, cm^2/g	$\mu_{\mathrm{Ag,i}}$, cm^2/g
Fe	0.34	0.88	8.07	7.11	6.40	70.46	358.97	18.40
Ni	0.41	0.88	7.85	8.33	7.48	91.77	59.58	24.19

Experiment 4. Verification of stoichiometry formula for superconducting materials.

First tested by **Oguzhan Can (SURF 2013)**

High energy superconductivity is studied in the lab experiment HTC http://www.physics.utoronto.ca/~phy326/htc/htc.pdf . Students create pellets of a superconductor material known as YBCO with the chemical formula $YBa_2Cu_3O_{7-x}$. The value of x is crucial. How the actual stoichiometry is close to the expected one will drastically effect the desired superconductive properties of the pellet. The powder for the pellet is a mixture of grinded Y_2O_3, $BaCO_3$ and CuO baked at $t^o > 900^oC$ in several cycles and then sintered in flowing oxygen. There are some other high temperature superconducting materials to study with their stoichiometry to be accurately defined. The spectrum of YBCO obtained in the Advanced labs in summer 2013 is demonstrated at the cover page of the Part II of the XRF experiment.

The XRF technique is a very good tool to find the solid sample composition if all x-ray emission peaks can be detected by the device. The apparatus in MP245 has a working energy range restricted to 2 keV < E < 50 keV. The lower energies are absorbed by air molecules and atoms of Be window that covers the input opening of the detector (see Fig. 2.5 on p.19 of this Manual). The energies higher than 50 keV are not excited by the primary source at 50 kV. However, the energies higher than 12 keV belong to the range with significant drop in the detector efficiency that must be taken into account for analysis of elements with Z > 35 using their K-series. Thus, the oxygen peak never appears in the spectrum. However, the peaks of all other elements of the superconducting substance can be identified and measured with confidence. Actually, the technique determines the amount of atoms of an element. Comparing the amounts of the components, an experimenter can find the stoichiometry formula of the substance making an estimate for the amount of oxygen.

The main objectives of this experiment are:

1. Derivation of analytical expression for calculating stoichiometry of YBCO, or $YBa_2Cu_3O_{7-x}$, basing on intensities of characteristic peaks of Y, Ba and Cu. Creating a Python code or any other software product for calculating the sample composition according to the derived equations.
2. Stoichiometry formula verification for YBCO in a pellet produced by students in the experiment HTC.
3. Determination of the unknown composition of a superconductor powder for the Condensed Matter Physics research group.

The two main problems in precise calculating the peak intensity are:
1 – existence of a background due to several different contributions [1]; and
2 – overlapping of the adjacent peaks.
Since the study of the physical origin of the spectrum background is not a priority goal of this experiment, you may work out a method of identifying the reference points in the spectrum that belong to purely background component, fitting the set of reference points with an appropriate function and subtracting the background from the original spectrum. An example of this method is shown in Fig. 4.1 for the YBCO sample. You may choose another approach to this problem.

The idea of processing the overlapping peaks is described on pp. 10-11 of this Manual.

For the main goal of this exercise, your determination of the characteristic peak intensity must be as precise as possible. This problem looks unresolvable since it is impossible to find the proper function $N_1(E)$ in the Eq.14 on p.9 of this Manual. However, the manufacturer of the x-ray tube introduced a piece of equipment that gives a reasonably accurate solution: there is a thin Al filter

inserted into our device between the source and the sample. Figure 4.2 gives an idea of the role of the filter.

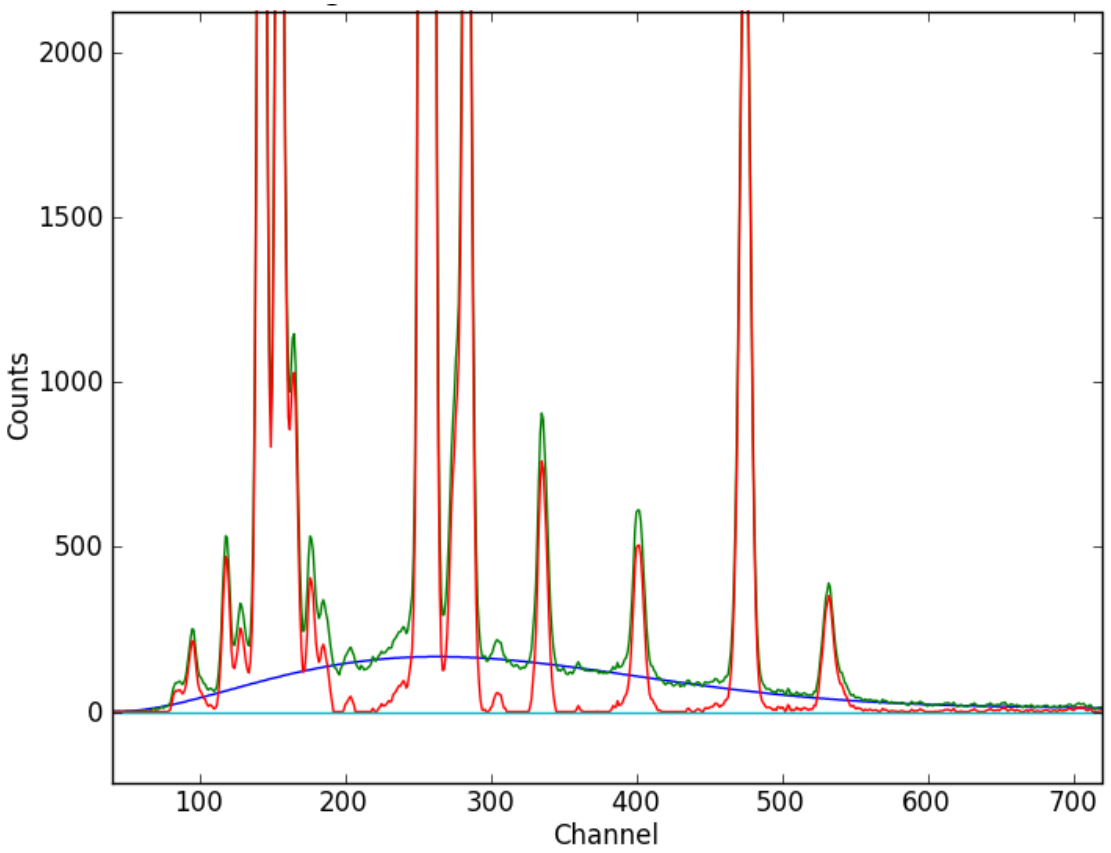

FIG.4.1: Spectrum of the YBCO sample before subtracting the background (green) and after subtracting the background (red). The polynomial function of the background (blue) is built through 9 reference points.

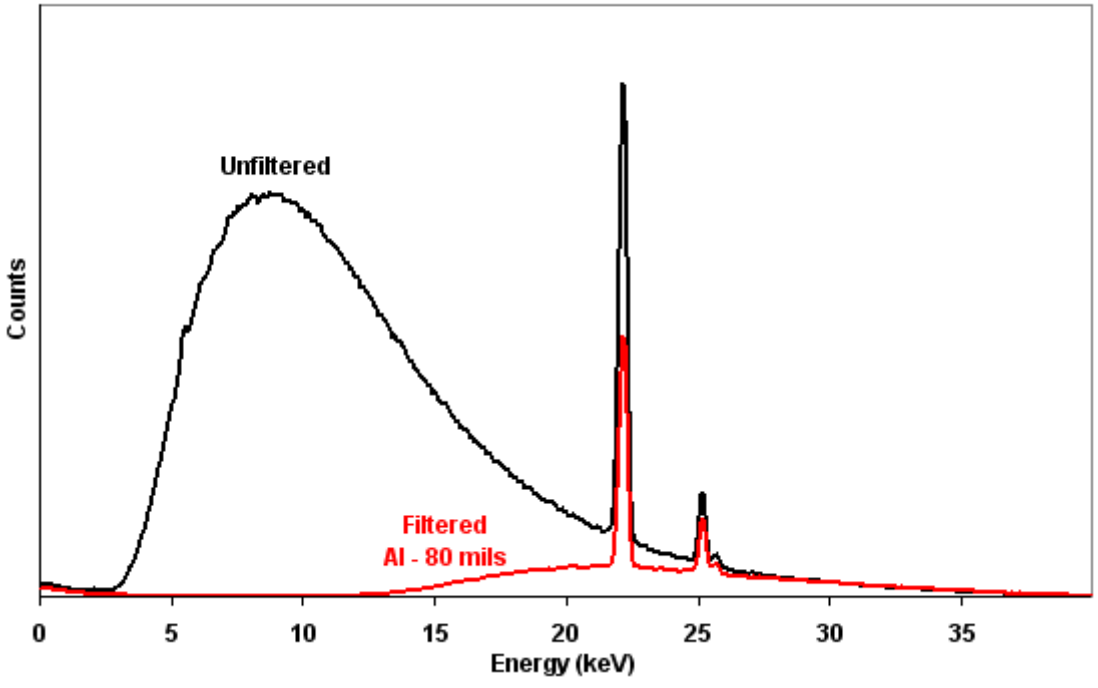

FIG. 4.2: MiniX-Ag output spectrum at 40 keV with and without 2-mm aluminum filter http://amptek.com/products/mini-x-ray-tube/#6 .

With aluminum filter inserted, we can consider the primary source spectrum being a spectrum of Ag K-series with a very good accuracy. This brings the Eq. 14 to

$$N_{i1} = \left(\frac{1}{\sqrt{2}} G\right) \cdot \left[\varepsilon_i \omega_i p_{tr,i} \left(1 - \frac{1}{r_i}\right)\right] \frac{\tau_{1i} C_i}{\sum \mu_{1j} C_j + \sum \mu_{ij} C_j} \cdot N_1 \qquad (4.1)$$

where absorption and attenuation coefficients of the primary radiation are related to the energy of Ag K_α line and N_1 is the intensity of the Ag K_α radiation from the x-ray tube in our apparatus. N_1 in the Eq.4.1 is a constant coefficient in the equation for any component.

Begin the experiment with taking spectra of a number of standard binary alloys containing Cu. The goal is to calibrate the spectrometer in units of "amount vs. intensity" for copper. You have a set of nine standard samples with the amount of Sn (tin) given in the Table 4.1.

TABLE 4.1. TYMETAL GA Series: Cu/Sn binary alloys which are used to prepare the basic calibration curve for Sn from 0% to 18%. Cu is the balance in all samples.

Standard	% Sn
GA1	2.31
GA2	3.95
GA3	5.78
GA4	8.25
GA5	9.96
GA6	12.27
GA7	13.94
GA8	16.18
GA9	18.10

We will consider that the amount of copper can be estimated as 100% - C_{Sn}. However, you will see the traces of other elements in the spectra and your records should show the entire composition of the sample at least qualitatively. Please guess on the uncertainty of the calibration procedure.

1. Choose the best settings for the MCA to take spectra of the given standard samples.
2. Using the ROI function of the MCA and varying the peak width, obtain the most accurate values of intensity of the Cu K_α peak in each sample. The position of this peak can be verified basing on your calibration, made in Part I of the experiment.
3. Use your own Python code or MATLAB to get more accurate results for the calibration curve "amount vs. intensity" for copper. A good option is to use a web page http://www.physics.utoronto.ca/~phy326/python/index.htm#Fitting on the Advanced Physics Laboratory web site with prepared Python codes. You should not expect a linear fit for your data.
4. For quantitative analysis of the YBCO pellet, take two-three spectra of this sample with same spectrometer settings as you used for calibration. With the ROI function of the MCA, obtain the most accurate values of intensity of the Cu K_α , Ba L_α and Y K_α peaks in the sample. The positions of the peaks can be verified basing on your calibration, made in Part I of the experiment.
5. Due to overlapping of some of the adjacent peaks, you have to accurately calculate their intensity, assuming that their position is a known quantity and their shape is a Gaussian curve. To *estimate* standard deviation of the Gaussian peaks, it is possible to take the half

of the value of FWHM (see the Glossary in Part I) considering it to be same for all the peaks. Actually, due to properties of the detector, the FWHM steadily increases with the increase of the energy of a peak. You must also account for the efficiency curve for the detector. The important information may be found in the Experiment II of this Manual in Fig.2.5 and Fig. 2.7. The greatest impact on the peak intensity is experienced by the Y K_α peaks, for which the detector efficiency drops by about 50%!

6. Using the calibration line for copper, find the amount of Cu in the YBCO pellet. Since the matrix effects are different in the Cu-Sn alloy and in the YBCO sample, your result is just the initial estimate of the copper amount.
7. The next step is to find the amount of the elements that have no standards, i.e. Ba and Y, using Eq. 4.1. The ratio of the Eq.4.1, written for two elements, one of which is Cu, gives a good estimate for the relative intensities of the components of the substance and, been re-organized, the relative concentration of the elements if the intensities are measured. On the other hand, we will assume that the sum of the concentrations is 100%. Equation 4.1 cannot be used directly to calculate the components concentration, but will demand an iteration procedure, because the values of attenuation coefficients and absorption coefficients contain the unknown concentration. You are expected to apply your skills in programming with Python and/or Matlab to compute.
8. Convert concentrations into stoichiometry indices and write the formula of the given YBCO substance. The best result obtained in the past was $Y_1Ba_2Cu_3O_{6.354}$ – with the greatest uncertainty for Y due to the lower detector response in this energy range.
9. Repeat steps 4, 5 and 7, 8 for the other superconducting material. There are no standard kits for all elements you can require for this analysis. As a single reference, it is possible to take a spectrum of one pure element (100% concentration) of any known component of the superconductor. The other difficulty is the sample preparation for materials that exist in a form of a powder. Report the stoichiometry formula for the unknown material and estimate the uncertainty of the method. You may find data on all superconductors on the web. Compare your formula to the expected one that you have found on the Internet.

All necessary data for this experiment are collected in Ref.[3, 4, 5] of the APPENDIX D and the "Other Resources" links on the web page http://www.physics.utoronto.ca/~phy326/xrf/index.htm

References

1. Horst Ebel. X-Ray Tube Spectra, X-Ray Spectrometry, **28**, 255-266 (1999)